

DEVELOPMENT OF POLYMER MATRIX COMPOSITES WITH TUNABLE
DIELECTRIC PROPERTIES

A THESIS SUBMITTED TO
THE GRADUATE SCHOOL OF NATURAL AND APPLIED SCIENCES
OF
MIDDLE EAST TECHNICAL UNIVERSITY

BY

NADİRE NAZLI ÖZKARAGÖZ

IN PARTIAL FULFILLMENT OF THE REQUIREMENTS
FOR
THE DEGREE OF MASTER OF SCIENCE
IN
METALLURGICAL AND MATERIALS ENGINEERING

FEBRUARY 2022

Approval of the thesis:

**DEVELOPMENT OF POLYMER MATRIX COMPOSITES WITH
TUNABLE DIELECTRIC PROPERTIES**

submitted by **NADİRE NAZLI ÖZKARAGÖZ** in partial fulfillment of the requirements for the degree of **Master of Science in Metallurgical and Materials Engineering, Middle East Technical University** by,

Prof. Dr. Halil Kalıpçılar
Dean, Graduate School of **Natural and Applied Sciences** _____

Prof. Dr. C. Hakan Gür
Head of the Department, **Metallurgical and Materials Eng.** _____

Prof. Dr. Arcan Fehmi Dericioğlu
Supervisor, **Metallurgical and Materials Eng., METU** _____

Examining Committee Members:

Prof. Dr. Caner Durucan
Metallurgical and Materials Eng., METU _____

Prof. Dr. Arcan Fehmi Dericioğlu
Metallurgical and Materials Eng., METU _____

Assist. Prof. Dr. Eda Aydoğan Güngör
Metallurgical and Materials Eng., METU _____

Assist. Prof. Dr. Simge Çınar Aygün
Metallurgical and Materials Eng., METU _____

Prof. Dr. Ziya Esen
Department of Inter-Curricular Courses, Çankaya University _____

Date: 08.02.2022

I hereby declare that all information in this document has been obtained and presented in accordance with academic rules and ethical conduct. I also declare that, as required by these rules and conduct, I have fully cited and referenced all material and results that are not original to this work.

Name, Last name : Nadire Nazlı Özkaragöz

Signature :

ABSTRACT

DEVELOPMENT OF POLYMER MATRIX COMPOSITES WITH TUNABLE DIELECTRIC PROPERTIES

Özkaragöz, Nadire Nazlı
Master of Science, Metallurgical and Materials Engineering
Supervisor : Prof. Dr. Arcan Fehmi Dericioğlu

February 2022, 68 pages

Ferroelectric materials are used in different applications because of their superior electrical and dielectric properties. Ferroelectric materials are polarized when an electrical field is applied to the material. This spontaneous polarization continues even if an electrical field is removed. BST (Barium Strontium Titanate) is one of the attractive ferroelectric materials which has a high dielectric constant and low dielectric loss tangent ($\tan\delta$). High dielectric constant and low loss tangent are necessary for tunable microwave applications, particularly at X/C band frequencies. Nevertheless, monolithic BST ceramic is not a proper material for electronic applications especially when conformality is required. To eliminate this deficiency of the BST ceramics, BST particle containing polymer matrix composites (BST/PS) providing unique properties can be developed. In the current study, effect of different parameters on the characteristics and tunability performance of the dielectric properties of the BST particle containing polymer matrix composites has been investigated. BST particle size, particle size distribution and content in the composites have been determined to be the key parameters effective on the tunability potential of such composites. Within the scope of this study, it was concluded that tunability potential of the BST/PS composites improves with increasing content of

the fine-sized BST ceramics having Ba/Sr/Ti molar ratio of 0.7/0.3/1 which increases further at higher applied bias voltage.

Keywords: BST, Ferroelectric Materials, Tunability

ÖZ

AYARLANABİLİR DİELEKTRİK ÖZELLİKLERE SAHİP POLİMER MATRİKSLİ KOMPOZİTLERİN GELİŞTİRİLMESİ

Özkaragöz, Nadire Nazlı
Yüksek Lisans, Metalurji ve Malzeme Mühendisliği
Tez Yöneticisi: Prof. Dr. Arcan Fehmi Dericioğlu

Şubat 2022, 68 sayfa

Üstün elektriksel ve yalıtım özelliklerinden dolayı ferroelektrik malzemeler farklı uygulamalarda kullanılmaktadır. Elektrik alan uygulandığında ferroelektrik malzemeler kutuplaşırlar. Bu anlık kutuplaşma elektrik alan uygulanması sona erdiğinde de devam eder. Baryum Stronsiyum Titanat yüksek dielektrik sabiti ve düşük dielektrik kaybı ile en ilgi çekici ferroelektrik malzemelerden biridir. Ayarlanabilir mikrodalga uygulamalarında özellikle X/C bandı frekanslarında, yüksek dielektrik sabiti ve düşük dielektrik kaybı gereklidir. Ancak BST seramiği bükülebilirlik gerektiren elektronik uygulamaları için uygun değildir. BST'nin bu özelliğini bertaraf etmek için eşsiz özelliklere sahip seramik parçacıklı polimer matrisli kompozit malzemeler geliştirilebilir. Bu çalışmada farklı parametrelerin BST polimer kompozitinin karakteristiğine ve dielektrik özelliklerinin ayarlanabilirlik potansiyeline etkisi incelenmiştir. Parçacık boyutu, parçacık boyutu dağılımı ve kompozitin içindeki BST miktarı, kompozitlerin ayarlanabilirlik potansiyeli için etkili temel parametrelerdir. BST/PS kompozitinin ayarlanabilirlik potansiyeli, kompozit içindeki ince boyutlu ve optimum kompozisyona sahip BST

parçacıkları arttıkça artmaktadır. Ayarlanabilirlik potansiyeli uygulanan voltaj değerindeki artış ile daha da artmaktadır.

Anahtar Kelimeler: BST, Ferroelektrik Malzemeler, Ayarlanabilirlik

To my beloved family

ACKNOWLEDGEMENTS

I would like to express my sincere gratitude to Prof. Dr. Arcan Dericiođlu for his guidance, support, understanding and encouragement throughout the study. He also helps to improve my scientific and academic thinking skills. I would also like to thank my committee members Prof. Dr. Caner Durucan, Prof. Dr. Ziya Esen, Assist. Prof. Dr. Eda Aydođan Gungör and Assist. Prof. Dr. Simge Cınar Aygün.

I thank my labmate Merve Özdil Darıcıođlu for her kind help and also members of the Electromagnetic Materials Laboratory for their guidance.

I am grateful to Volkan Kalender, the head of my division in TÜBİTAK SAGE, for his understanding, support and positive attitudes throughout the study. Also, special thanks to my colleagues from TÜBİTAK SAGE for their support and help.

I also thank my best friends Betül Aydın, Ayşenur Ahsen and Merve Tahran for their valuable support in my entire life. They have always been there for me through thick and thin.

Finally, I am deeply grateful to my family for providing me with unconditional support, continuous encouragement, love and guidance throughout my life. Any of the accomplishments would not have been possible without them.

TABLE OF CONTENTS

| | |
|--|-------|
| ABSTRACT..... | v |
| ÖZ | vii |
| ACKNOWLEDGEMENTS | x |
| TABLE OF CONTENTS..... | xi |
| LIST OF TABLES | xiii |
| LIST OF FIGURES | xiv |
| LIST OF ABBREVIATIONS | xvii |
| LIST OF SYMBOLS | xviii |
| CHAPTERS | |
| 1 INTRODUCTION | 1 |
| 2 LITERATURE REVIEW | 5 |
| 2.1 Ferroelectricity and Ferroelectric Materials | 5 |
| 2.1.1 Barium Strontium Titanate..... | 6 |
| 2.1.2 Production Methods of Barium Strontium Titanate..... | 8 |
| 2.2 Barium Strontium Titanate/Polymer Composites | 9 |
| 2.2.1 Theoretical Dielectric Constant Models for Composites..... | 10 |
| 2.2.1.1 Logarithmic Model (Lichtenecker Model) | 10 |
| 2.2.1.2 Modified Lichtenecker Model | 11 |
| 2.2.1.3 Maxwell-Garnett Model | 11 |
| 2.3 Tunability | 12 |
| 2.3.1 Tunability Measurement Techniques..... | 14 |
| 2.3.2 Tunable Devices..... | 17 |

| | | |
|-------|---|----|
| 3 | EXPERIMENTAL PROCEDURE..... | 21 |
| 3.1 | General Procedure..... | 21 |
| 3.2 | Sample Preparation | 22 |
| 3.2.1 | Production of Barium Strontium Titanate Powders by Solid-State Reaction..... | 22 |
| 3.2.2 | Fabrication of BST/PS Composites for Microwave Frequency Applications..... | 23 |
| 3.3 | Characterization | 24 |
| 3.3.1 | Microstructural Characterization..... | 24 |
| 3.3.2 | Particle Size Analysis | 24 |
| 3.3.3 | Phase Analysis..... | 25 |
| 3.3.4 | Optical Characterization | 25 |
| 3.3.5 | Dielectric Characterization..... | 25 |
| 3.3.6 | Tunability Measurements | 26 |
| 4 | RESULTS AND DISCUSSION..... | 29 |
| 4.1 | Morphology of the Synthesized BST Powders..... | 29 |
| 4.2 | Particle Size Analysis of BST Powders..... | 32 |
| 4.3 | XRD Analysis of BST Powders..... | 33 |
| 4.4 | Optical Characterization of BST/PS Composites | 36 |
| 4.5 | Dielectric Characterization of BST/PS Composites | 42 |
| 4.6 | Tunability Potential of BST/PS Composites | 48 |
| 5 | CONCLUSION | 55 |
| | REFERENCES | 61 |

LIST OF TABLES

TABLES

| | |
|---|----|
| Table 3.1. List of BST/PS composites processed in this study..... | 24 |
|---|----|

LIST OF FIGURES

FIGURES

| | |
|--|----|
| Figure 2.1. Hysteresis loop for a ferroelectric material in an electric field [8]. | 5 |
| Figure 2.2. Perovskite crystal structure of Barium Strontium Titanate [16]. | 7 |
| Figure 2.3. Current materials' tunability and dielectric constant values [16]. | 12 |
| Figure 2.4. Tunability of BST ceramics for different grain sizes [20]. | 13 |
| Figure 2.5. Measurement setup [39]. | 15 |
| Figure 2.6. Reflection IDC on sapphire substrate [46]. | 15 |
| Figure 2.7. Measurement method of BST IDC [43]. | 16 |
| Figure 2.8. Measurement setup with VNA and two WR-90 waveguides [48]. | 16 |
| Figure 2.9. Measurements of tunable components with G-S-G probe [49]. | 17 |
| Figure 2.10 Using of one tunable filter instead of few filter banks [51]. | 18 |
| Figure 2.11 BST/Polymer based phase shifter [34]. | 18 |
| Figure 3.1. Measurement setup for dielectric characterization. | 26 |
| Figure 3.2. Experimental setup for tunability measurements. | 27 |
| Figure 3.3. The composite tape. | 27 |
| Figure 4.1. Morphology of BST powders a) 0.7/0.3/1 Ba/Sr/Ti (ball mill), b) 1/1/1 Ba/Sr/Ti (ball mill), c) 0.7/0.3/1 Ba/Sr/Ti (centrifugal mill) and d) 1/1/1 Ba/Sr/Ti (centrifugal mill). | 30 |
| Figure 4.2. Morphology of BST powders a) 0.7/0.3/1 Ba/Sr/Ti (ball mill), b) 1/1/1 Ba/Sr/Ti (ball mill), c) 0.7/0.3/1 Ba/Sr/Ti (centrifugal mill) and d) 1/1/1 Ba/Sr/Ti (centrifugal mill). | 31 |
| Figure 4.3. Particle size analysis of BST powders with a) 1/1/1 Ba/Sr/Ti ratio and b) 0.7/0.3/1 Ba/Sr/Ti ratio. | 33 |
| Figure 4.4. XRD patterns of BST (0.7/0.3/1) powders produced by a) centrifugal milling and b) ball milling. | 34 |
| Figure 4.5. XRD patterns of BST (1/1/1) powders produced by a) centrifugal milling b) ball milling. | 35 |
| Figure 4.6. Visual appearance of a) pristine PS polymer tape b) composite with 5% BST and c) composite with 10% BST (for ball milled BST (0.7/0.3/1)). | 36 |

| | |
|---|----|
| Figure 4.7. Transmittance (%) of pristine PS polymer tape and composites with 5% and 10% as a function of wavelength (for ball milled BST (0.7/0.3/1))..... | 37 |
| Figure 4.8. Visual appearance of a) pristine PS polymer tape b) composite with 5% BST and c) composite with 10% BST (for ball milled BST (1/1/1)). | 38 |
| Figure 4.9. Transmittance (%) of pristine PS polymer tape and composites with 5% and 10% as a function of wavelength (for ball milled BST (1/1/1))..... | 39 |
| Figure 4.10. Visual appearance of a) pristine PS polymer tape b) composite with 5% BST and c) composite with 10% BST (for centrifugal milled BST (0.7/0.3/1)). | 40 |
| Figure 4.11. Transmittance (%) of pristine PS polymer tape and composites with 5% and 10% as a function of wavelength (for centrifugal milled BST (0.7/0.3/1)). | 40 |
| Figure 4.12. Visual appearance of a) pristine PS polymer tape b) composite with 5% BST and c) composite with 10% BST (for centrifugal milled BST (1/1/1)).... | 41 |
| Figure 4.13. Transmittance (%) of pristine PS polymer tape and composites with 5% and 10% as a function of wavelength (for centrifugal milled BST (1/1/1)).... | 42 |
| Figure 4.14. Transmission losses (S ₁₂) of BST/PS composites with a) ball milled BST powders and b) centrifugal milled BST powders. | 43 |
| Figure 4.15. Reflection losses (S ₂₂) of BST/PS composites with a) ball milled BST powders and b) centrifugal milled BST powders. | 44 |
| Figure 4.16. Dielectric constants of BST/PS composites with a) ball milled BST powders and b) centrifugal milled BST powders. | 46 |
| Figure 4.17. Loss tangent of BST/PS composites with a) ball milled BST powders and b) centrifugal milled BST powders. | 47 |
| Figure 4.18. Change in reflection loss (S ₂₂) of 5 wt% ball milled BST (0.7/0.3/1) containing composite under 0, 100 and 150 V bias voltage. | 49 |
| Figure 4.19. Change in reflection loss (S ₂₂) of 10 wt% ball milled BST (0.7/0.3/1) containing composite under 0, 100 and 150 V bias voltage. | 49 |
| Figure 4.20. Change in reflection loss (S ₂₂) of 5 wt% ball milled BST (1/1/1) containing composite under 0, 100 and 150 V bias voltage. | 50 |

| | |
|---|----|
| Figure 4.21. Change in reflection loss (S22) of 10 wt% ball milled BST (1/1/1) containing composite under 0, 100 and 150 V bias voltage..... | 51 |
| Figure 4.22. Change in reflection loss (S22) of 5 wt% centrifugal milled BST (0.7/0.3/1) containing composite under 0, 100 and 150 V bias voltage..... | 52 |
| Figure 4.23. Change in reflection loss (S22) of 10 wt% centrifugal milled BST (0.7/0.3/1) containing composite under 0, 100 and 150 V bias voltage..... | 52 |
| Figure 4.24. Change in reflection loss (S22) of 5% centrifugal milled BST (1/1/1) containing composite under 0, 100 and 150 V bias voltage..... | 53 |
| Figure 4.25. Change in reflection loss (S22) of 10% centrifugal milled BST (1/1/1) containing composite under 0, 100 and 150 V bias voltage..... | 54 |

LIST OF ABBREVIATIONS

ABBREVIATIONS

RoHS: Restriction of the Use of Certain Hazardous Substances

XRD: X-Ray Diffraction

SEM: Scanning Electron Microscope

UV-VIS Spectrophotometer: Ultraviolet Visible Spectrophotometer

PS: Polystyrene

PVDF: Polyvinylidene Fluoride

DC: Direct Current

RF: Radio Frequency

MIM: Metal-Insulator-Metal

LIST OF SYMBOLS

SYMBOLS

μm : micrometer

nm: nanometer

GHz: GigaHertz

ϵ : Dielectric Constant (Permittivity)

T_c : Curie Temperature

CHAPTER 1

INTRODUCTION

Everyday technological requirements are changing and increasing in line with the demands of the developing world. The need for tunable devices arises from the absence of devices which can be used both at microwave and radio frequency bands with adjustable properties.

Main component of tunable devices are ferroelectric materials. Barium Strontium Titanate (BST) ceramic is one of the most preferred ferroelectric materials which has superior dielectric properties such as high dielectric constant and low dielectric loss along with being electrically insulating even at microwave frequency bands [1]. BST is commonly used in electronic applications such as voltage-tunable capacitors, phase shifters, tunable filters, oscillators etc. [2]. Being a ceramic material BST is rigid and brittle in monolithic form with several restrictions in processing. These limitations restrict the integration of BST ceramics in some applications. To overcome these limitations, alternatively BST ceramic particles can be incorporated in polymer matrices to obtain composite materials usable in various electronic applications. Polymers have acceptable thermal properties and mechanical strength along with chemical inertness, flexibility and also low loss tangent [3]. Therefore ceramic particle and polymer matrix combinations have the potential of providing outstanding properties. Different polymers such as PVDF, silicon-rubber, polyimide, polyvinylchloride, polystyrene and polyurethane are being used as the matrix of the composites used in electronic applications [4].

Different production methods are available for synthesizing of BST ceramic particles. Sol-gel method, hydrothermal method, RF sputtering [1], pulsed laser deposition [5], metal-organic solution deposition [6] and finally solid-state reaction production methods have been used generally. All production methods have specific

pros and cons. Choosing of one of these methods depends on the requirements of the specific application.

The solid-state reaction method is preferred for obtaining micron to nano size powders without needing to complicated equipment. This method includes mixing of raw materials with milling followed by calcination and sintering stages. Final powders are homogeneous and have small particle sizes.

The purpose of this study was to obtain BST/polymer composites which can be used at high frequency applications. In addition, tunability potential of the composites which corresponds to the adjustability of their dielectric properties under applied electric field has been studied. The main aim here is to obtain materials available for electronic applications alternately functional at multiple frequency bands. Investigation of the dielectric properties of the BST ceramics at high frequencies was done, and these properties were also investigated under applied DC bias voltage. To accomplish of this goal, BST micro-nano particles were produced with solid-state reaction method by using two different milling methods. BST particles were characterized using XRD (X-ray Diffraction) to observe the formation of phases and their crystallinity, while SEM (Scanning Electron Microscope) analysis was used to investigate the morphology of the particles. BST particles were also investigated with particle size analysis which provided significant information about powder size and distribution.

BST particles were incorporated in polystyrene (PS) matrix and BST/PS composites having two different particle contents (5 and 10 wt%) were obtained by tape casting. Particle distribution in the composites was characterized using UV-VIS spectrophotometer which provided transmittance of the composite tapes in the wavelength range of 300-800 nm. Electromagnetic wave transmission and reflection response of the composites was characterized by free space method in 2-18 GHz frequency range. Dielectric properties of the composites were extracted from the measured transmission and reflection losses.

Effect of BST quantity on the dielectric properties of the composites was investigated. Besides this, effect of particle size and particle distribution on the dielectric performance of the composites were evaluated. Furthermore, different bias voltage values were applied to the composites and effect of these parameters on the tunability potential of BST/PS composites were examined.

In the following section (Chapter 2), brief literature review which includes short explanations about ferroelectricity and ferroelectric materials, properties of Barium Strontium Titanate ceramics and their production methods, BST/PS composites and finally about tunability and tunable devices has been presented. Chapter 3 compasses materials which were used for experimental studies and also techniques which were preferred for the production and characterization of the materials. In the Results and Discussion chapter SEM images, particle size analysis, XRD patterns, light transmittance results, dielectric characterization results and finally tunability potential measurement results are presented and discussed. Finally, significant inferences of the study are given in the Conclusions.

CHAPTER 2

LITERATURE REVIEW

2.1 Ferroelectricity and Ferroelectric Materials

Ferroelectric materials exhibit spontaneous polarization although an external electric field is removed. The relative permittivity of these materials is larger than other insulators so they are used mostly at capacitors. An external electric field is applied to the material, permanent dipoles of the ferroelectric materials are aligned with the external electric field direction. After all dipoles are aligned with this direction, a saturation of the polarization is accomplished. Even if the external field is removed, polarization remains which is called remanent polarization. Remanent polarization is only withdrawn with reverse electric field is applied to the material. When applying a reverse electric field to the material, the hysteresis loop given in Figure 2.1 is obtained [7].

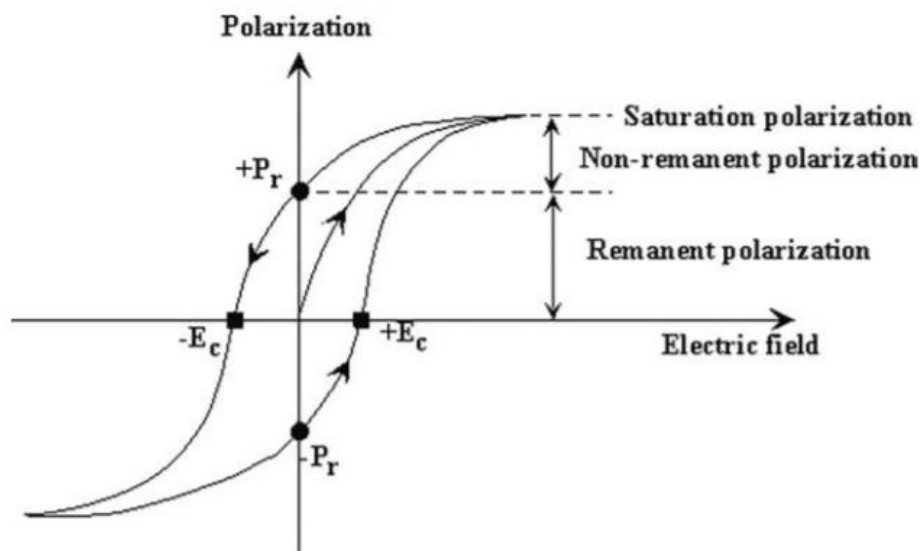


Figure 2.1. Hysteresis loop for a ferroelectric material in an electric field [8].

Ferroelectrics have two classes which are order-disorder type and displacive type. Ordering of ions provides former type ferroelectricity as in the hydrogen bounded KH_2PO_4 . Displacive type ferroelectricity is related to the displacement of crystal sublattices in relation with others. Such as perovskite crystals, ferroelectricity is a displacive type [9].

The temperature, which is called Curie temperature, is an important for ferroelectrics. At above that temperature, the ferroelectricity of material destroys. Above Curie temperature, material becomes paraelectric which means the external electric field can not affect the material [7]. Curie temperature can be adjusted with compositional changes which will be explained further.

2.1.1 Barium Strontium Titanate

Barium Titanate had first discovered. Among other ferroelectric materials, Barium Titanate is shown an important discovery because of its composition and structure, other ferroelectrics, which had found before BT, include hydrogen bonds but BT does not. Another difference from other ferroelectrics is BT's ferroelectric phases are more than one [8]. Pure BT has more than one phase transition temperatures; at 120°C paraelectric to ferroelectric phase transition occurs as from cubic to tetragonal, around 5°C from tetragonal to orthorhombic and the other appear [10]. BT and its solid solutions have a wide range of dielectric constant value from hundreds to thousands. The reason for that wide range is adjustability of dielectric constant with lots of parameters such as amount of doping, microstructure (grain size, density) depending on production method, temperature and external electric field which is applied to BT [11]. Doping is an effective and commonly used method to change dielectric constant of BST [12,13].

Barium Strontium Titanate was discovered later. The addition of Strontium to the Barium Titanate has advantages on the material. Strontium provides a decrease in

the Curie temperature. The Curie temperature of material declines to almost room temperature with addition enough amount of Strontium. Then BST can be used at room temperature with the highest dielectric constant since the dielectric constant goes up near Curie temperature. Strontium also causes a drop in dielectric constant value. Some applications require a low dielectric constant because of diminishing dielectric loss of material at high frequencies [14,15].

Dielectric loss at high frequencies is a major problem for tunable devices. Dielectrics have complex permittivity values which consist of the real and imaginary part. Real part means energy storage in the material, on the contrary, the imaginary part shows the dissipation of energy. Loss tangent is found by the dividing imaginary part of dielectric constant by the real part. Loss is the tangent of the angle between the loss component and storage component. The origin of the intrinsic loss is the energy exchange between the external electromagnetic (EM) wave and the vibration of the ions of the material [9].

Both Barium Titanate and Strontium Titanate have perovskite crystal (ABO_3) structures, which have TiO_6 octahedron at the center of the cubic structure [2]. The perovskite structure's ionic arrangement is given in Figure 2.2 [16].

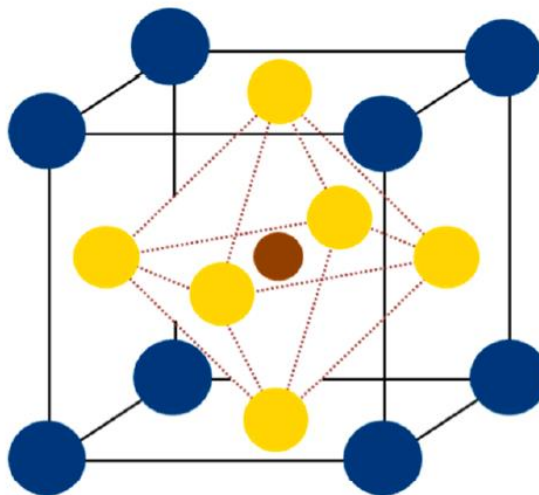


Figure 2.2. Perovskite crystal structure of Barium Strontium Titanate [16].

Above Curie temperature, BST has a cubic crystal structure which causes no spontaneous polarization. There is no net charge between negative and positive ions because of the central symmetry of oxygen octahedron within the cubic crystal structure.

When below the Curie temperature, BST has tetragonal structure and Ti ions of oxygen octahedra do not preserve balanced position and form strong dipoles. Spontaneous polarization appears along the Ti cations' direction [16].

Barium Strontium Titanate is one of the ferroelectric materials which is frequently used at capacitors, tunable devices, varactors, phase shifters, tunable antennas, phased array antennas. Using of BST for tunable applications has become widespread in recent years. The use of lead in electronic and microelectronic devices has been forbidden by the European directive RoHS since July 2014. Therefore, BST is preferred instead of lead-containing ferroelectrics [17].

2.1.2 Production Methods of Barium Strontium Titanate

A number of methods, from simplest to complex ones, are available to synthesize BST. Choosing of production methods depends on the applications since products are different from each other for every method. Nano- or micron- size powder form, platelet form, fiber form or thin film form on a substrate with nanometer thickness can be obtained from different methods.

Generally used production methods are mixed-oxide [18–21], sol-gel [22–26], spin coating [27], screen printing [17], thin film production methods [28,29] etc. One of the most preferred methods is a sol-gel method. Sol-gel is a low temperature process that mainly consists of transforming one step to another: micron size particles in liquid (sol) to macro material (gel) [23].

Thin films of BST are widely used for especially electronic components. Thin film production methods compass lots of challenging steps. First of all, substrate selection is important for the coating process. Polymeric substrates are not proper for high

temperature thin film coating process. On the other hand, ceramic substrates limit the application areas. Even if the proper substrate is found, other stages continue to be challenging. Forming shape on thin film is another hard step called photolithography. Some applications require more than one photolithography step. The thin film fabrication process necessitates specialty for every stage of the coating and coating material. Finally, the film microstructure, film-substrate interface, morphology of the film must be optimized for good performance [6].

Screen printing [30] and inkjet printing [31] are new methods for the production of components that have complex shapes. Lots of factors must be controlled for good printing. The viscosity of the ink is an important parameter for printing. Before printing, adjustability of BST particles with optimum composition is necessary. The substrate is also significant for these processes. After printing, curing is required for ink so substrate should be chosen with considering curing temperature [32].

Among the other production methods, the solid-state reaction is the simplest one [16]. Compared to other methods, there are no extra requirements for this method. Raw materials of this method are Barium Carbonate, Strontium Carbonate and Titanium Dioxide. Ball milling and centrifugal milling are done for mixing and reducing particle size. Raw materials, ethanol and zirconium oxide balls are mixed in a nylon jar by a planetary ball mill. Then drying of the mixture is done. Powders are formed as pellets and pellets are sintered at 1200⁰C to 1500⁰C for 3 h [20]. The mixed oxide method is commonly used for obtaining the final products with uniform particle distribution and smaller particle sizes.

2.2 Barium Strontium Titanate/Polymer Composites

Barium strontium titanate is a versatile ceramic component of high frequency devices with good electrical properties [3]. However, BST is generally used as thick and thin films, and these films are brittle and rigid. Consequently, these films are improper for flexible and conformal devices [33]. Polymers have good thermal,

chemical and mechanical properties. Also, some polymers have a low dielectric loss [3]. Polymers' such properties and BST's deficiencies were considered together and 0-3 type BST/Polymer composites have been begun to use to overcome problems of ceramic films. Phases that have dimensions in composites are marked as 0-1-2-3 in a diphasic system. 0-3 type composite is generally used in which 0 and 3 denote filler and matrix phases which means three-dimensional polymer matrix with ceramic particles [16]. BST/polymer composites are produced by mixing micro-sized powder and nano-sized powder with polymer [4,34].

Different polymers are used as matrices. Cyclic olefin copolymer was used as a matrix extensively at researches [35,36]. COC is a thermoplastic polymer that has low loss tangent values at high frequencies and high glass transition temperature, 133⁰C [33]. Besides COC, acrylonitrile butadiene styrene [37], low density polyethylene [38], polyphenylene sulfide [3], polyvinylidene fluoride [39,40] and polystyrene [41] were used as polymer matrix.

Polystyrene is an easily found polymer which can be shaped with injection molding or extruding. The ease of processability of PS provides to produce different shapes of composites even complex shapes. Other reasons for using PS as a matrix are good thermal and mechanical stability, ease of machinability, low dielectric loss [41].

2.2.1 Theoretical Dielectric Constant Models for Composites

2.2.1.1 Logarithmic Model (Lichtenecker Model)

The logarithmic model is related to the volume of a component in composites. The dielectric constant of composite is extracted from the rate of volume of the constituents of composites. The formula of this model is given below:

$$\log \varepsilon = \vartheta_p \log \varepsilon_p + \vartheta_c \log \varepsilon_c \quad \text{[Equation 2.1]}$$

ε is the relative permittivity of composite, ϑ_p and ϑ_c are volume fractions of polymer and ceramics, ε_p and ε_c are relative permittivities of polymer and ceramics [3].

Dielectric constants of components should be close to each other for the use of this model.

2.2.1.2 Modified Lichtenecker Model

Although Lichtenecker Model is proper for composites with low ceramic content, developed model has been used for composites with high ceramic loading which is the Modified Lichtenecker Model. This model is applicable up to 75% volume fraction of ceramic:

$$\log \varepsilon = \log \varepsilon_p + \vartheta_c(1 - k) \log \frac{\varepsilon_c}{\varepsilon_p} \quad [\text{Equation 2.2}]$$

where k assumes as 0.3 for good dispersion of particles in composites. This model is also used for differences of dielectric constants of components are large [16].

2.2.1.3 Maxwell-Garnett Model

Maxwell-Garnett Model provides accurate results about the permittivity of composites. This model considers the effect of the shape of the filler of composites. Model is merely valid for spherical particles [16,35].

$$\varepsilon = \varepsilon_p \left[1 + \frac{3\vartheta_c(\varepsilon_c - \varepsilon_p)}{(1 - \vartheta_c)(\varepsilon_c - \varepsilon_p) + 3\vartheta_p} \right] \quad [\text{Equation 2.3}]$$

Theoretical models give general information about final products' dielectric properties. However, experimental results are diverse from theoretical calculations since theoretical models' assumptions do not match real situations. In real situations,

contrary to assumptions, inhomogeneous distribution of particles in matrix or agglomerations of particles occur that causes deviations from theoretical calculations.

2.3 Tunability

Tunability can be defined as a change in permittivity of material under an applied electric field [9]. Material with a high dielectric constant provides high tunability. However, microwave applications require low dielectric constant values with high tunability. Current studies focus on high dielectric constant with high tunability which is shown at Figure 2.3 whereas low permittivity, which should be less than 100, with high tunability is required for high frequency applications [16].

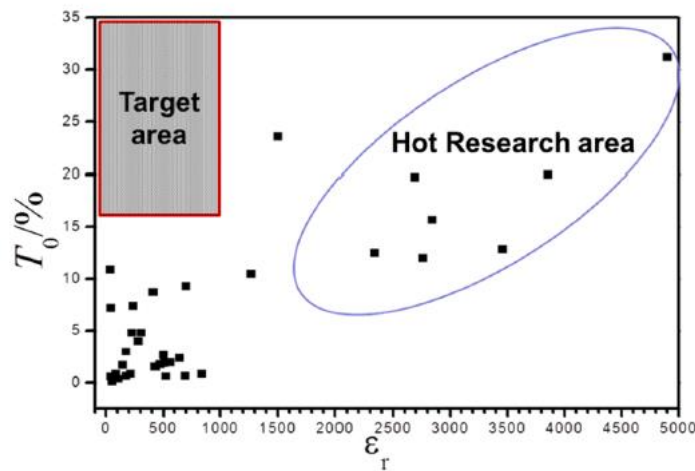


Figure 2.3. Current materials' tunability and dielectric constant values [16].

Tunability of the dielectric properties can be controlled by different stimuli. DC bias voltage is one of the fundamental extrinsic factors for tunability. Tunability increases with high voltage values [11]. High voltage is not proper for most of the applications, so new methods have been developed for lowering the required bias voltage values. Bulk BST requires high voltage in order to generate high electric field. However, thin films need a lower voltage value to form a high electric field and also high

tunability [42]. Although dielectric constant increases with thickness, thin films are preferred for microwave tunable applications [1]. Grain size of the BST is another parameter for tunability of the material. Grain size is dependent on the production methods and final grain size is important for tunability performance. Grain size of about 10 μm has been reported to provide best tunability performance. Comparison of tunability of BST ceramics with different grain sizes is shown in Figure 2.4 as a function of applied bias voltage. Grain size is controlled by annealing temperature of films. Grain size increases when sintering temperature is high enough [20].

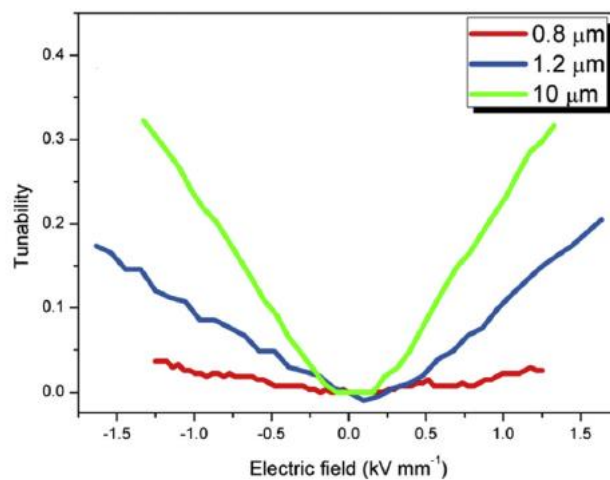


Figure 2.4. Tunability of BST ceramics for different grain sizes [20].

Another noteworthy situation related to tunability is BST phase distribution in composite. In another words, tunability of the dielectric properties arises from BST phase in composites. Continuous phase of BST provides higher tunability [36]. Tunability enhances with voltage gradually yet after critical voltage value, which is called threshold bias, tunability increases sharply [16].

Tunability is defined in two different ways: First is related to capacitance value. Change in capacitance to zero-bias capacitance value gives tunability [43]. Another calculation is related to permittivity of material. Change in the permittivity divided by the zero-bias permittivity provides tunability of material [44, 45].

Tunability formula is given by:

$$\tau = \frac{C(E_0) - C(E_v)}{C(E_0)} = \frac{\varepsilon(E_0) - \varepsilon(E_v)}{\varepsilon(E_0)} \quad [\text{Equation 2.4}]$$

where $C(E_0)$ and $\varepsilon(E_0)$ are zero-bias capacitance and zero-bias permittivity, respectively, while $C(E_v)$ and $\varepsilon(E_v)$ are capacitance and permittivity under bias-field, respectively.

2.3.1 Tunability Measurement Techniques

Tunability measurements are quite complex. For tunability measurements, conductivity is necessary. For thin film's tunability measurements, there must be bottom and top electrodes which are conductive materials. These electrodes are coated bottom and top of the film so a metal-insulator-metal structure is obtained and measurements are realized with these contacts [46,47]. MIM (Metal-Insulator-Metal) structures decrease voltage values for tunability [47].

One of the schematic measurement setups for tunability is shown in Figure 2.5. Vector Network Analyzer provides to obtain return losses and insertion losses of material in broad frequency range MHz to GHz. DC power supply provides high voltages to material and measurements can be done under the electrical field. Two 10 dB directional couplers are used for isolation up to 2 kV. Two DC blocks are used for additional protection to obtain precise measurements [39].

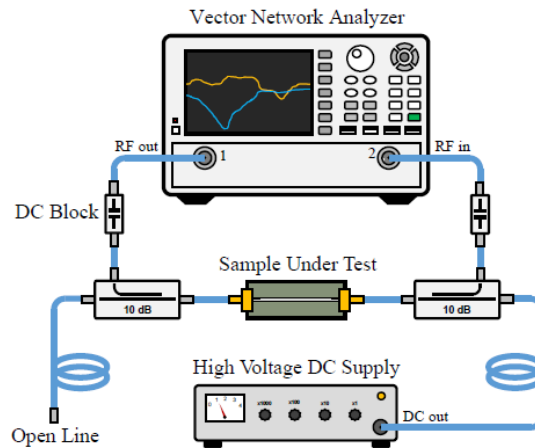


Figure 2.5. Measurement setup [39].

Metal-ferroelectric-metal capacitor configuration is an alternative way for tunability measurements. Capacitance values of material are measured under applied electrical field with Network Analyzer [47].

Interdigitated capacitor is also used configuration for tunability measurement of BST films. BST is coated on the sapphire substrate by RF sputter. The lift-off process is realized for obtain IDC configuration which is shown in Figure 2.6. Measurements are done with Vector Network Analyzer with TRL calibration [46].

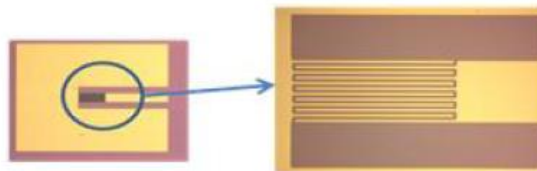


Figure 2.6. Reflection IDC on sapphire substrate [46].

Tunability measurement method of BST IDCs on Liquid Crystal Polymer is shown in Figure 2.7. Measurement is carried out from 10 MHz to 50 GHz with maximum 200 V [43].



Figure 2.7. Measurement method of BST IDC [43].

The waveguide measurement method is used to obtain more precise results than open space method. BST based frequency selective surface is placed between two waveguides for measurements which can be seen in Figure 2.8 [48].

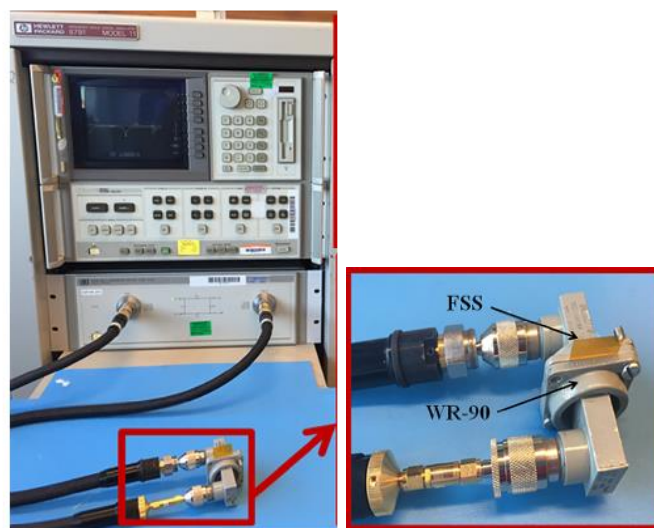


Figure 2.8. Measurement setup with VNA and two WR-90 waveguides [48].

DC voltage is applied to one of the FSS side with power source, other side of FSS is grounded. Then measurements are performed from 0 V to maximum 240 V [35].

An in-house complementary split ring resonator (CSRR) transmission line sensor is used for the tunability measurements. Silver coated BST pellets are placed on the CSRR transmission line sensor and the two port S parameters are obtained using Vector Network Analyzer. DC voltage is applied in the range of -850 V to 850 V with 25 V incremental steps. 10 s measurement time is necessary for devices to record data [20].

Another measurement method is carried out using G-S-G probe. One probe measurements are done for varactors and two probe measurements are done for phase shifters. The voltage power supply is attached to the varactors via Bias tees. For phase shifters' tunability measurements, voltage is directly applied to the phase shifter using bias network. This setup is given in Figure 2.9 [49].

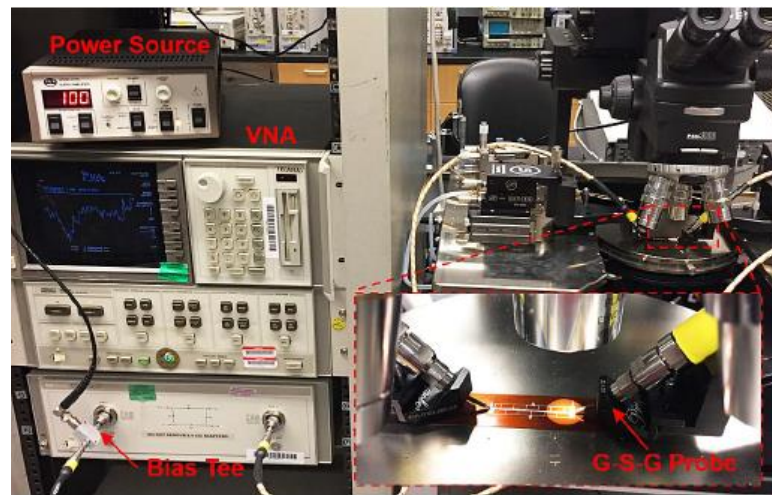


Figure 2.9. Measurements of tunable components with G-S-G probe [49].

2.3.2 Tunable Devices

Tunable devices have been used in recent applications because of its crucial role at microwave frequency range. Tunable devices are phase shifters [34], varactors [50],

phased array antennas, frequency selective surfaces [48], band-pass filters [51], tunable antennas [52] etc. These devices include BST or other ferroelectric materials in different forms for tunability. The dependency of the dielectric constant on the electrical field provides freedom to device developers. Tunability of the dielectric properties provides a decrease in the components of the whole system as shown in Figure 2.10. The antenna's operating frequencies are determined by loaded capacitor value but thin film varactor is integrated to the antenna, an antenna can be reconfigurable. BST enhances the performances of tunable devices with a widening frequency range of work. BST/polymer composites can be integrated even in complex shapes which is also beneficial for antenna design. One of the tunable components of the conformal antennas, phase shifter, can be seen in Figure 2.11. Phase shifter is used to electronically alter the RF signal's phase angle [34].

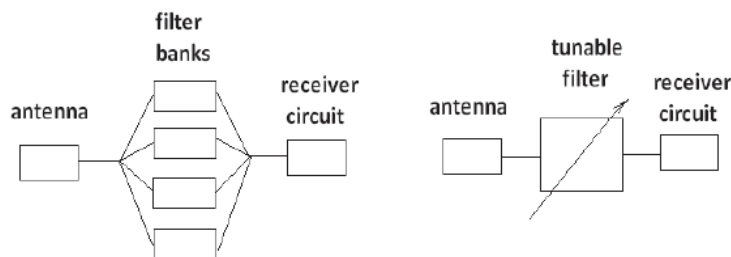


Figure 2.10 Using of one tunable filter instead of few filter banks [51].

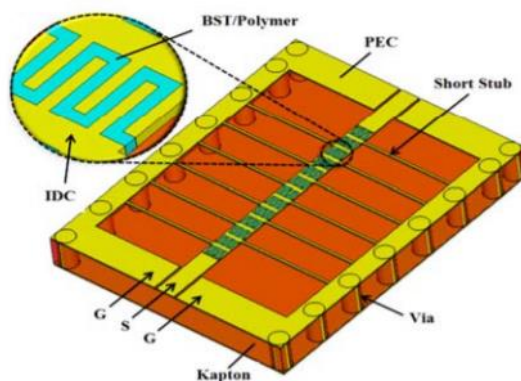


Figure 2.11 BST/Polymer based phase shifter [34].

Ferroelectric materials should be met below requirements of tunable devices;

- Low loss tangent
- Proper permittivity (less than 500)
- High dielectric tunability of the dielectric properties (max 50%)
- Low leakage current/strong insulator (10^{11} ohm-cm) [6].

CHAPTER 3

EXPERIMENTAL PROCEDURE

3.1 General Procedure

Barium Strontium Titanate (BST) powders were synthesized to be incorporated as filler material in polymer matrix composites. The solid-state reaction method was used for the production of BST powders. Milling is done to obtain homogeneous mixing and to reduce particle size. Two different milling methods have been used which are conventional and centrifugal milling. According to previous studies [49,53] when the Barium to Strontium molar ratio is 0.7/0.3, optimum electrical properties are obtained from this ceramic. Therefore, this study focuses on this particular composition. For verification of this composition, another Barium to Strontium molar ratio which is 1/1 was also produced and its properties have been compared with those of the optimum composition. The solid-state reaction method includes calcination and sintering steps which were realized between 900-1100⁰C [18].

After completion of powder production, composite fabrication was conducted which is composed of mixing polymer solution with the synthesized powders. This homogeneous mixture was processed as composite tapes by tape casting. Consequently, a polymer matrix composite has been fabricated.

Average particle size and particle size distribution of the synthesized BST powders were found by particle size analyzer (Mastersizer 2000, Malvern Instruments Ltd.,UK). Particle size and its distribution were confirmed by Scanning Electron Microscope (Nova 430 NanoSEM) images. In addition, particle morphology was obtained by SEM. An X-ray diffractometer (Miniflex, Rigaku, Japan) was used for phase analysis.

The transmittance of light through the composite tapes was measured with UV-VIS Spectrophotometer (Perkin Elmer Lambda 35 UV-VIS Spectrophotometer). Transmission data displayed the distribution of particles in the matrix indirectly. Dielectric properties were characterized by free space method using a Vector Network Analyzer (VNA, Anritsu 37269E, Japan) in the 2-18 GHz. Tunability measurements were done by applying DC voltage to the composite tapes using a power supply within the free space setup attached to the Vector Network Analyzer.

3.2 Sample Preparation

3.2.1 Production of Barium Strontium Titanate Powders by Solid-State Reaction

A solid-state reaction was used for the production of BST powders. BaCO₃ (Merck), SrCO₃ (Merck) and TiO₂ (Merck) were used as raw materials. These materials were mixed in BaCO₃/SrCO₃/TiO₂ molar ratios of 0.7/0.3/1 and 1/1/1. Weighed materials were put in the ball milling cup, and then zirconia balls and isopropyl alcohol were added to this mixture. Ball milling process was applied to materials at 375 rpm for 7 h. The ball to raw material weight ratio was chosen as 100/12 during the process. After ball mill, the mixture was put in the drying oven at 50⁰C and drying was done for 24 h. Then, dried powders were compacted as pellets applying 40 bar of pressure. Pellets were exposed to calcination process at muffle furnace. For the calcination process each pellets were held at 3 different temperatures of 900⁰C, 1000⁰C and 1100⁰C in a sequential manner where they were soaked at each temperature for ~2 h. After the calcination process, the sintering stage was conducted at 1100⁰C for 3 h. Total time spent for calcination and sintering process was approximately 14 h.

Besides the conventional ball milling process, the new and speedy method was used for mixing and reducing particle size which is centrifugal mixing. Centrifugal mixing was realized by the centrifugal mixer (Thinky mixer ARE-250, Japan) with zirconia balls as the milling medium. During this process chosen ball to raw material weight

ratio was 100/12 and milling time was 2 min. In the presence of a milling medium centrifugal mixing combines high speed mixing (2000 rpm) and planetary mixing. Planetary mixing term comes from the mixing process similar to the planet's rotation. The planet rotates both around itself and around the sun and centrifugal mixing occurs exactly in that way.

Finally, after two different mixing processes and all of the heating processes were conducted, BST powders with 2 different chemical compositions were obtained. These powders were unsurprisingly different from each other. Conventional ball milling products had larger average particle size than centrifugal milled ones.

3.2.2 Fabrication of BST/PS Composites for Microwave Frequency Applications

Polystyrene (PS) was selected as the matrix material of the composites in this study. First of all, polystyrene was dissolved in the proper solvent. Aromatic hydrocarbons are chosen for the dissolution of this type of thermoplastics. Xylene (Merck) was used as a solvent for this study. The weight ratio of PS/Xylene was 25/100. Xylene and PS were weighed and stirred with a magnetic stirrer for 2 h. After the homogeneous solution had been obtained, BST powders were added to the solution in 2 different amounts which are 5 and 10 wt%, and the mixing process continued with the magnetic stirrer for 1 more hour. After the completion of the mixing process the mixture was poured on the tape caster. The blade passed over the mixture, and composite tapes were obtained. The list of composites containing BST powders with 2 different compositions obtained by 2 different milling methods composition which were formed by the tape casting process are given in Table 3.1.

Table 3.1. List of BST/PS composites processed in this study.

| BST/PS Composite Designation # | Composition of the BST Powders | Milling Methods of BST Powders | wt% BST Powder in Composite |
|--------------------------------|--------------------------------|--------------------------------|-----------------------------|
| 1 | 0.7/0.3/1:Ba/Sr/Ti | Centrifugal Milling | 5 wt% BST |
| 2 | 0.7/0.3/1:Ba/Sr/Ti | Centrifugal Milling | 10 wt% BST |
| 3 | 0.7/0.3/1:Ba/Sr/Ti | Ball Milling | 5 wt% BST |
| 4 | 0.7/0.3/1:Ba/Sr/Ti | Ball Milling | 10 wt% BST |
| 5 | 1/1/1:Ba/Sr/Ti | Centrifugal Milling | 5 wt% BST |
| 6 | 1/1/1:Ba/Sr/Ti | Centrifugal Milling | 10 wt% BST |
| 7 | 1/1/1:Ba/Sr/Ti | Ball Milling | 5 wt% BST |
| 8 | 1/1/1:Ba/Sr/Ti | Ball Milling | 10 wt% BST |

3.3 Characterization

3.3.1 Microstructural Characterization

Particle size, distribution and morphology of BST powders were investigated by Scanning Electron Microscope (Nova 430 NanoSEM). There was neither sample preparation nor coating step for this observation. Low voltage and low vacuum conditions were used during examination to prevent charging.

3.3.2 Particle Size Analysis

Particle size analysis was done to observe particle size and distribution of BST powders. Particle size analysis was carried out with particle size analyzer (Mastersizer 2000, Malvern Instruments Ltd.,UK). Hydrous method was used for analysis, and water was used as dispersant. Measurement range of the device was 10 nm to 3000 μm .

3.3.3 Phase Analysis

An X-ray diffractometer (Miniflex, Rigaku, Japan) was used for phase analysis. XRD analysis using Cu K α source having K α 1=1.54056 Å and K α 2=1.5444 Å wavelengths was realized between 10⁰ to 90⁰. Scan speed and step width were 1⁰/min and 0.02⁰, respectively. The diffractometer was operated at 40kV and 15mA. The scanning mode of the diffractometer was continuous. The goniometer of the X-ray diffractometer was MiniFlex 300/600. A standard sample holder was used during the measurements. Sample preparation was not required for this analysis.

3.3.4 Optical Characterization

Optical characterization of the BST/PS composite tapes was conducted with UV-VIS Spectrophotometer (Perkin Elmer Lambda 35 UV-VIS Spectrophotometer). Light transmittance of the composite tapes has been measured between 300 nm and 800 nm. Tapes were cut to a minimum size of 15×15 mm for the measurements. Pristine PS tape was used as the reference sample during the measurements. 8 measurements were done for 8 different samples. Additionally, composites were photographed above the light source, and the distribution of the BST particles in the composites was examined with the unaided eye.

3.3.5 Dielectric Characterization

Dielectric properties of the BST/PS composites were characterized by free space setup attached to a Vector Network Analyzer (VNA, Anritsu 37269E, Japan) which is shown in Figure 3.1. Used free space setup is capable of operating from 2 to 18 GHz frequencies. Nevertheless, the measurements were conducted in 8-12 GHz range (X-band) in order to concentrate to the frequencies widely used in numerous applications. For the measurements, composite tapes were cut to samples 10×10 cm in size. The tapes were attached to in-house 3D printed plastic frames to stabilize

them and to prevent their bending during the free space measurements. After sample preparation, measurements were conducted on 8 different composite tapes using the setup seen in Figure 3.1. Results of these measurements were reported in the form of reflection loss (S_{11} , S_{22}) and transmission loss (S_{21} , S_{12}) values (S parameters). By using the measured reflection and transmission loss values post-processing was conducted. Post-processing constitutes extracting dielectric constant and loss tangent values of the composites from the measured reflection and transmission characteristics. Dielectric constant and loss tangent were obtained with the aid of MATLAB software by using a matlab code pre-designed for this purpose using the Nicholson-Ross-Weir (NRW) algorithm [54-56].



Figure 3.1. Measurement setup for dielectric characterization.

3.3.6 Tunability Measurements

The tunability of the composite tapes was measured by the above-mentioned setup. However, in this case free space setup measurements were conducted under DC bias voltage which was applied by a home-built experimental setup (Figure 3.2). Direct current supply provided voltage to the composite tapes (Figure 3.3) and adjustability

of their dielectric properties was recorded at different applied voltage values. For these measurements, the tapes were prepared to provide an electrical contact. Silver ink was applied to the edge of the tapes. Prepared tapes were placed in the free space setup holder. Positive and negative ends of the power supply were attached to the conductive ink applied edges of the tapes. Then 100V and 150 V of bias voltage was applied to composite tapes sequentially. Changes in the dielectric properties were obtained by post-processing the measurement results under bias voltage.

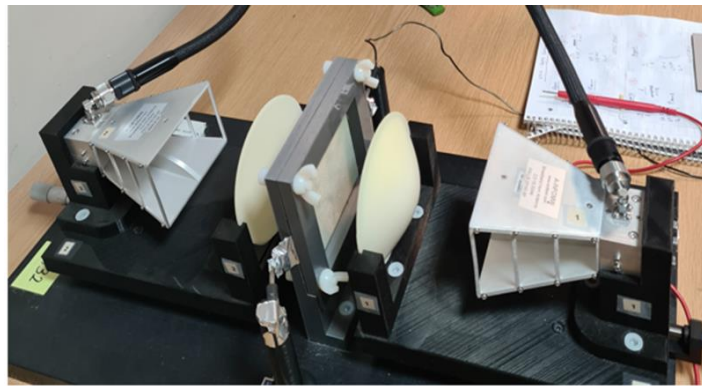


Figure 3.2. Experimental setup for tunability measurements.



Figure 3.3. The composite tape.

CHAPTER 4

RESULTS AND DISCUSSION

4.1 Morphology of the Synthesized BST Powders

Morphology of the synthesized BST powders was observed by Scanning Electron Microscope. Independent of the milling method used powders having a Ba/Sr/Ti molar ratio of 0.7/0.3/1 in their composition showed spherical-like morphology as can be seen in Figure 4.1 a) and c). However, particles with a Ba/Sr/Ti molar ratio of 1/1/1 displayed irregular shaped morphology with larger size Figure 4.1 b) and d). Powders produced by the centrifugal milling have an average size of ~300 nm, while those produced by conventional ball milling have particle sizes varying from 300 nm to 1 μm . Moreover, as seen in Figure 4.1 a) and b) ball milled BST powders of either composition reveal an agglomerated structure.

Figure 4.2 displays similar results with Figure 4.1, where the morphology of the synthesized BST powders is shown at a higher magnification (x30000) in some more details. It is clearly seen that conventional ball milling results in larger particle size with a more agglomerated structure as compared to centrifugal milling for both chemical compositions.

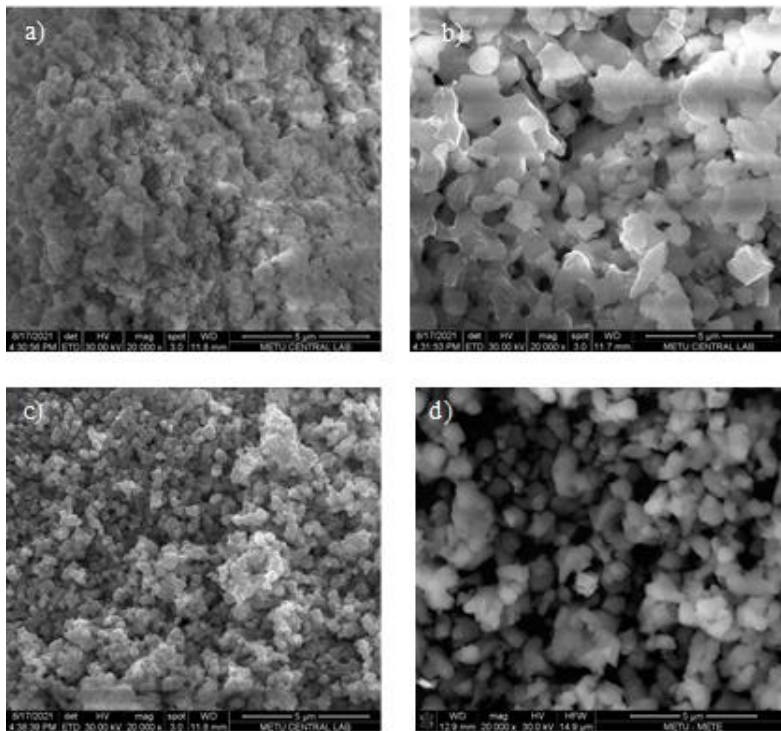


Figure 4.1. Morphology of BST powders a) 0.7/0.3/1 Ba/Sr/Ti (ball mill), b) 1/1/1 Ba/Sr/Ti (ball mill), c) 0.7/0.3/1 Ba/Sr/Ti (centrifugal mill) and d) 1/1/1 Ba/Sr/Ti (centrifugal mill).

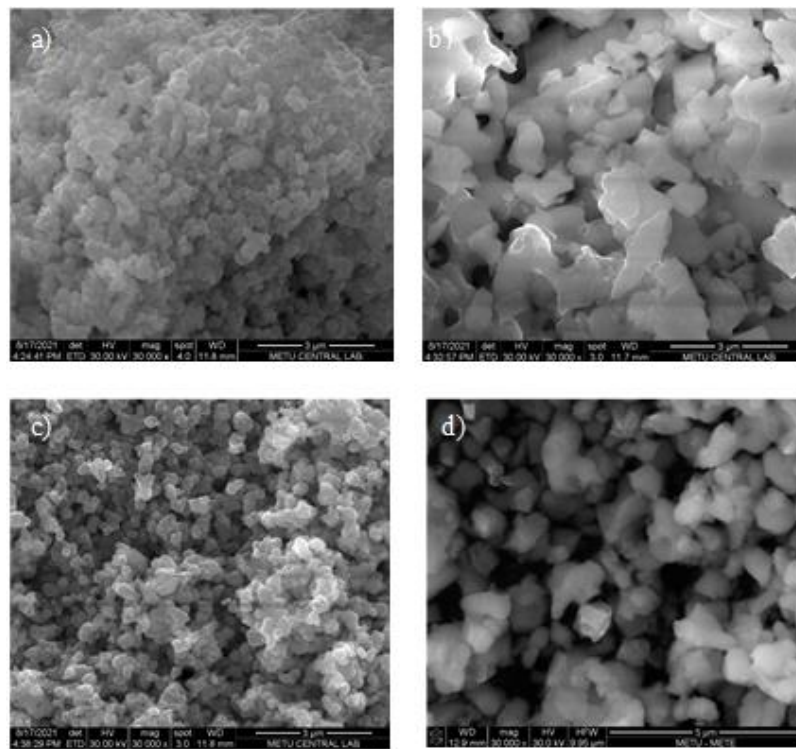


Figure 4.2. Morphology of BST powders a) 0.7/0.3/1 Ba/Sr/Ti (ball mill), b) 1/1/1 Ba/Sr/Ti (ball mill), c) 0.7/0.3/1 Ba/Sr/Ti (centrifugal mill) and d) 1/1/1 Ba/Sr/Ti (centrifugal mill).

4.2 Particle Size Analysis of BST Powders

Particle size analysis was done to determine particle size reduction achieved by conventional ball milling and centrifugal milling processes. As shown in Figure 4.3 a), the average particle size of the BST powder with a Ba/Sr/Ti molar ratio of 1/1/1, which was fabricated by ball milling, is approximately 1 μm . Particle size analysis also shows the distribution of particle size. According to Figure 4.3 a), intensification of particle size for ball milled powders is seen to be between 1 and 10 μm with an inhomogeneous, bimodal size distribution. On the contrary, ball milled BST powder with a Ba/Sr/Ti molar ratio of 0.7/0.3/1 shows a smaller average particle size with more homogenous distribution (Figure 4.3 b)). Difference in the particle size and distribution between these two ball milled products can be attributed to the fact that BST powder with 1/1/1 Ba/Sr/Ti ratio included more hydrous components than that of 0.7/0.3/1 Ba/Sr/Ti ratio resulting in agglomeration and larger particle sizes with inhomogeneous size distribution.

Figure 4.3 a) and b) shows that the particle size of powders produced by centrifugal milling is in the range of 250-300 nm. Larger particles were eliminated by this method. Centrifugal milling has proven its efficiency in terms of providing finer particle sizes with more homogeneous particle size distribution where the milling time was in minutes order. Conventional ball milling can also be an alternative way to reduce particle size, yet a considerably longer operation time exceeding 5-10 h is required for this method. According to results demonstrated in Figure 4.3 b), fine particle sizes and homogeneous size distribution can also be obtained by ball milling similar to centrifugal milling under the condition that enough ball milling time in the order of multiple hours is applied as opposed to centrifugal milling which provides these results in minutes.

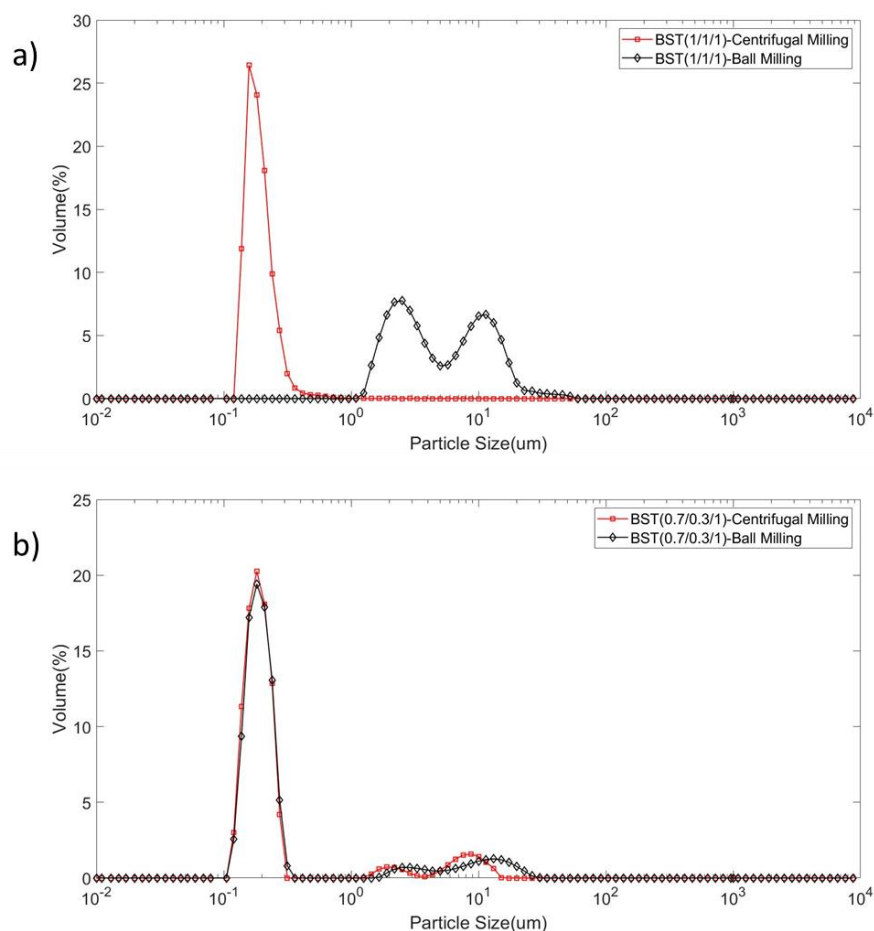


Figure 4.3. Particle size analysis of BST powders with a) 1/1/1 Ba/Sr/Ti ratio and b) 0.7/0.3/1 Ba/Sr/Ti ratio.

4.3 XRD Analysis of BST Powders

XRD data showed the phases present in the synthesized powders. According to XRD patterns in Figure 4.4, independent of the milling method $\text{Ba}_{0.67}\text{Sr}_{0.33}\text{TiO}_3$ phase appeared in the structure of the powders where no residual BaCO_3 , SrCO_3 or TiO_2 seems to be remaining from the raw materials. Although both patterns shown in Figure 4.4 are similar in appearance, unlike the centrifugal milled powder, peaks in the pattern of the ball milled powder have a slight deviation from those of the standard $\text{Ba}_{0.67}\text{Sr}_{0.33}\text{TiO}_3$.

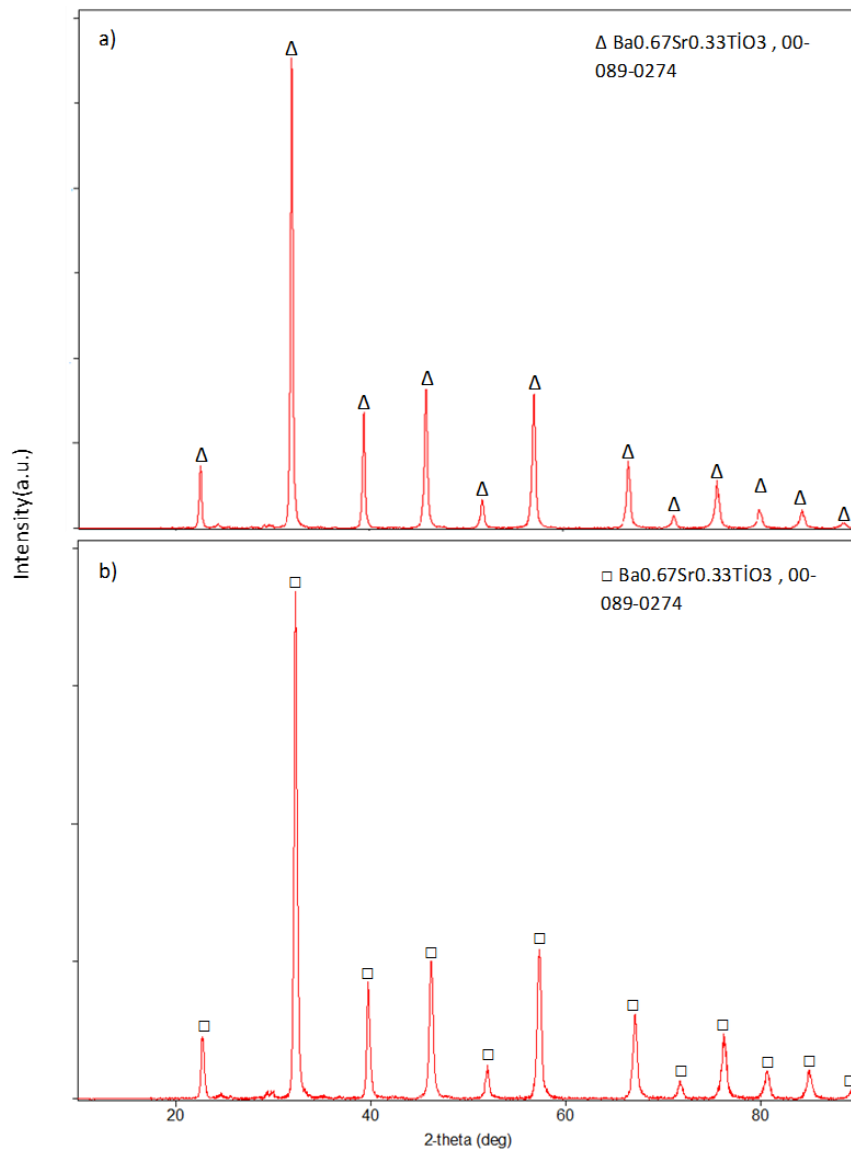


Figure 4.4. XRD patterns of BST (0.7/0.3/1) powders produced by a) centrifugal milling and b) ball milling.

Composition of the BST powder is critical on the phases forming in the structure. In the BST powder with 1/1/1 Ba/Sr/Ti ratio, existence of the $\text{Ba}_{0.67}\text{Sr}_{0.33}\text{TiO}_3$ phase is not expected. Two different phases are detected in the XRD patterns which are Ba_2TiO_4 and $(\text{SrO})_2\text{TiO}_2$ (Figure 4.5). Presence of barium titanate and strontium titanate separately in the ceramic do not provide optimum dielectric properties for the material. Room temperature paraelectric phase is not possible with the presence of these two phases leading to poor dielectric performance in the material. High

degree of crystallinity is another criterion for obtaining desired dielectric properties. Consequently, it has been observed that these requirements are not met with BST powder having 1/1/1 Ba/Sr/Ti ratio.

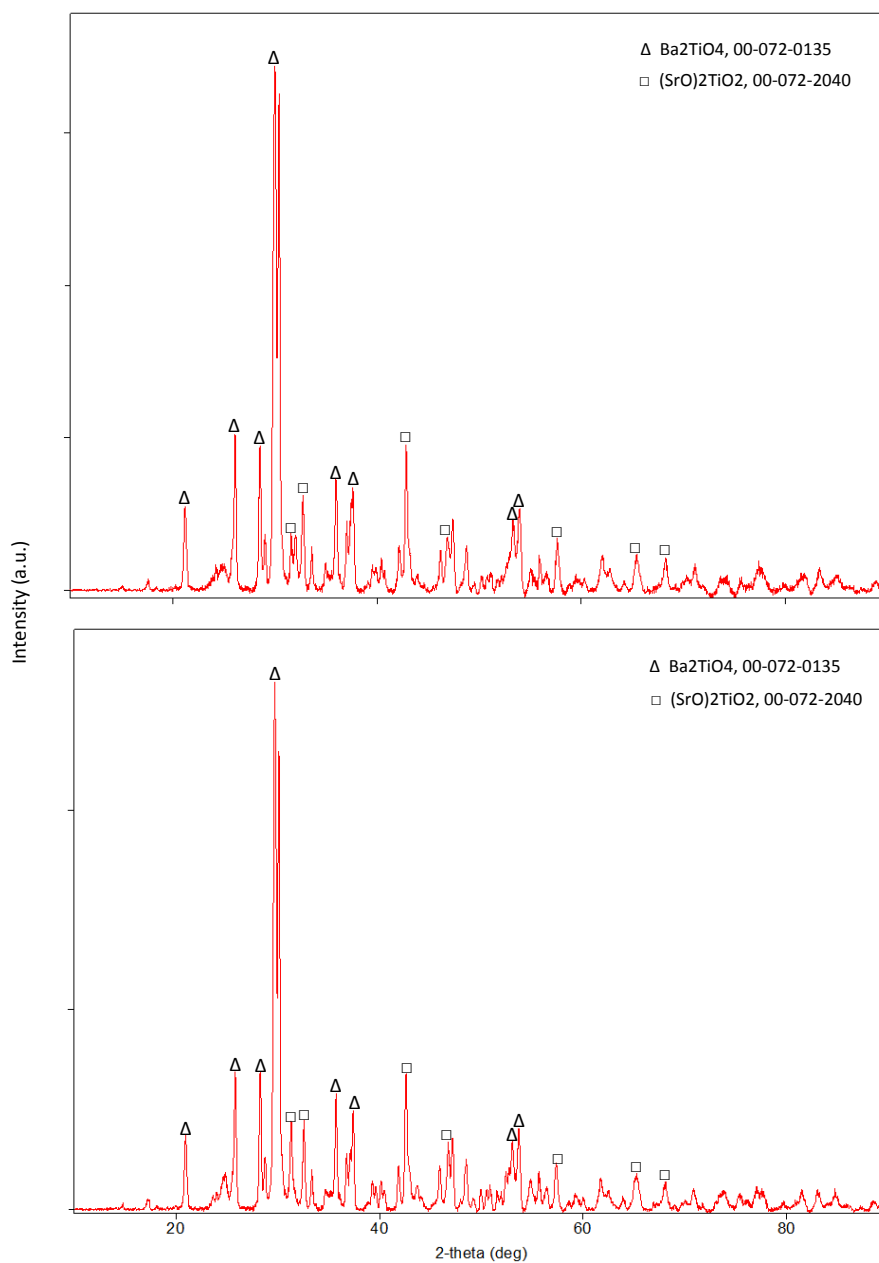


Figure 4.5. XRD patterns of BST (1/1/1) powders produced by a) centrifugal milling b) ball milling.

4.4 Optical Characterization of BST/PS Composites

Quantity of light which passes through material is called transmittance. Visible light transmittance of the pristine PS matrix as well as that of BST/PS polymer composites with 2 different BST content has been measured by UV-VIS Spectrophotometer. Light transmittance measurements were realized between 300 and 800 nm wavelengths. Purpose of this measurement was to somehow compare the distribution of the BST particles in the polymer composites. Composites with higher particle loading showed lower visual light transmittance (Figure 4.6). There seems to be no obviously visual brightness heterogeneity on the composite surfaces pointing out to relatively uniform particle distribution within the composites.

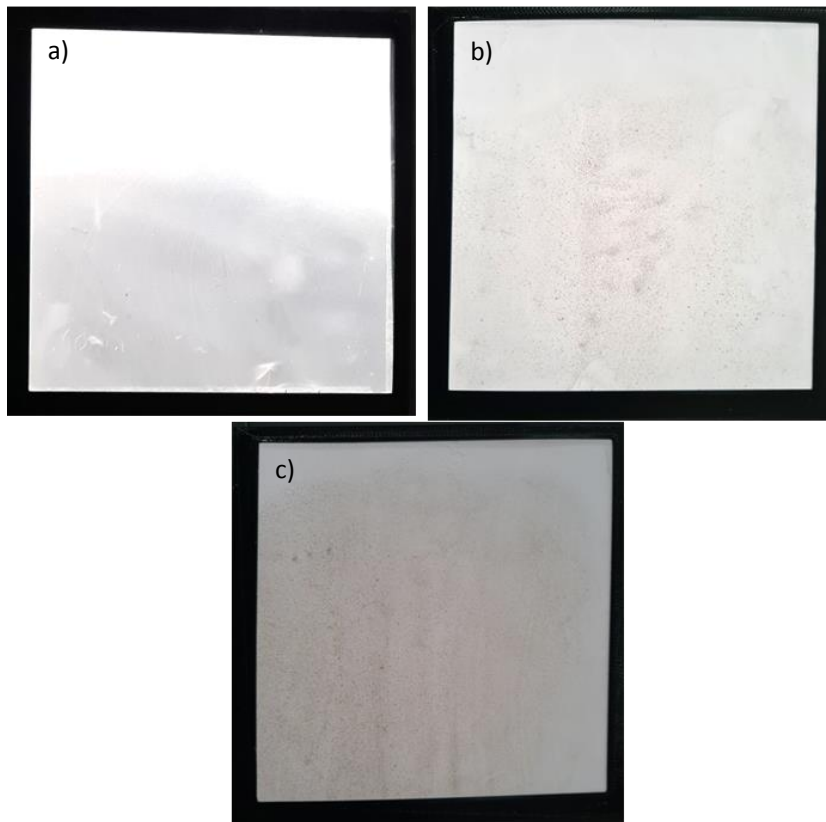


Figure 4.6. Visual appearance of a) pristine PS polymer tape b) composite with 5% BST and c) composite with 10% BST (for ball milled BST (0.7/0.3/1)).

Spectroscopic light transmittance values of the composites (Figure 4.7) are in good accordance with their appearance, where brighter appearance of the pristine PS gets darker while its light transmittance decreases with increasing BST powder content. That is to say Figure 4.6 and Figure 4.7 support each other about the light transmittance of the materials. Image of the pristine PS matrix without BST particles is the brightest, where it gradually becomes darker for the composite tapes with 5% and 10% BST particles, respectively. Transmittance results of the materials seen in Figure 4.7. According to Figure 4.7, highest transmittance value belongs to monolithic PS polymer matrix, as there are no obstacles for light transmission. Transmittance drops to lower values for composites with BST particles. Almost 70% decrease in transmittance has been seen for the composites. Composite with higher BST particle content has less transmission value as shown in Figure 4.7. These results give an information about the distribution of the particles in the composites. Both visual appearance and spectroscopic light transmittance results for the composites with 5% and 10% BST particles provide verification for relatively uniform distribution of the particles in the composites.

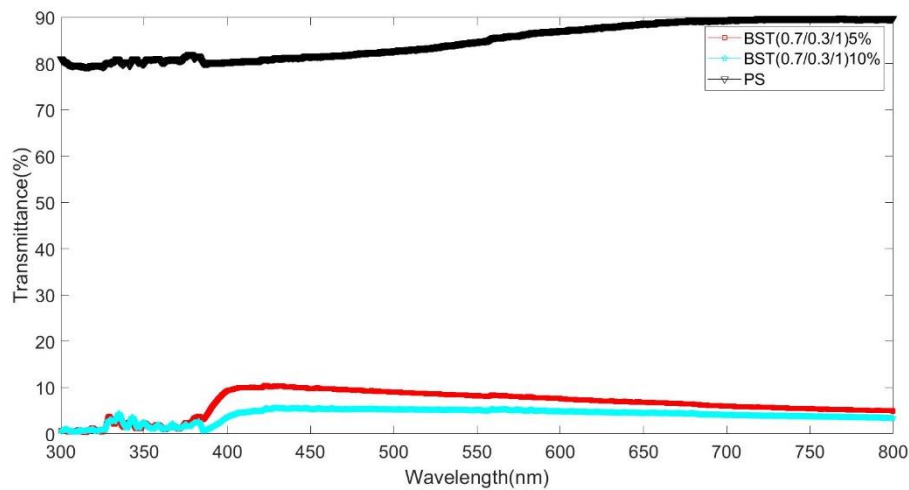


Figure 4.7. Transmittance (%) of pristine PS polymer tape and composites with 5% and 10% as a function of wavelength (for ball milled BST (0.7/0.3/1)).

Comparison of the results presented in Figure 4.8 and Figure 4.9 reveals that above-mentioned discussion also prevails for the visual appearance, light transmittance, and hence uniform particle distribution of the composites containing ball milled BST (1/1/1) powders. Additionally, it is seen in Figure 4.9 that light transmittance of the composites with ball milled BST (1/1/1) powders is almost half those of the composites with ball milled BST (0.7/0.3/1) for the respective powder contents. This is due to the fact that BST (1/1/1) powders produced by ball milling have higher average particle sizes and agglomerations as discussed and presented previously in Figures 4.1, 4.2 and 4.3. Higher amount of light transmittance is observed with higher particle size for the same powder content, as less surface coverage of the agglomerated particles corresponds to less scattering and hence more transmission through the material.

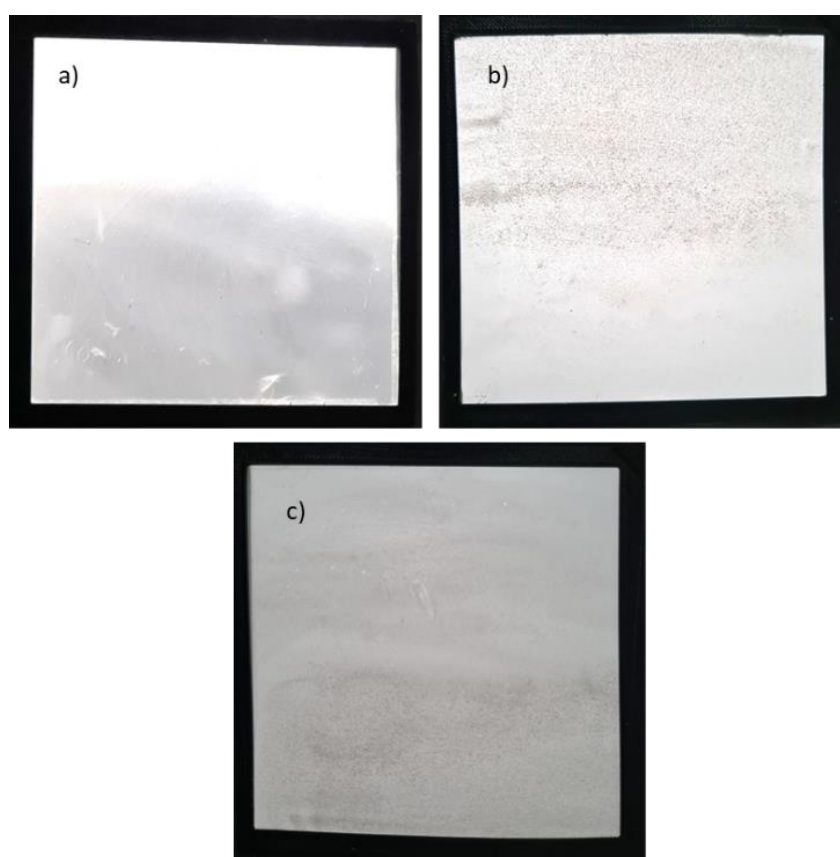


Figure 4.8. Visual appearance of a) pristine PS polymer tape b) composite with 5% BST and c) composite with 10% BST (for ball milled BST (1/1/1)).

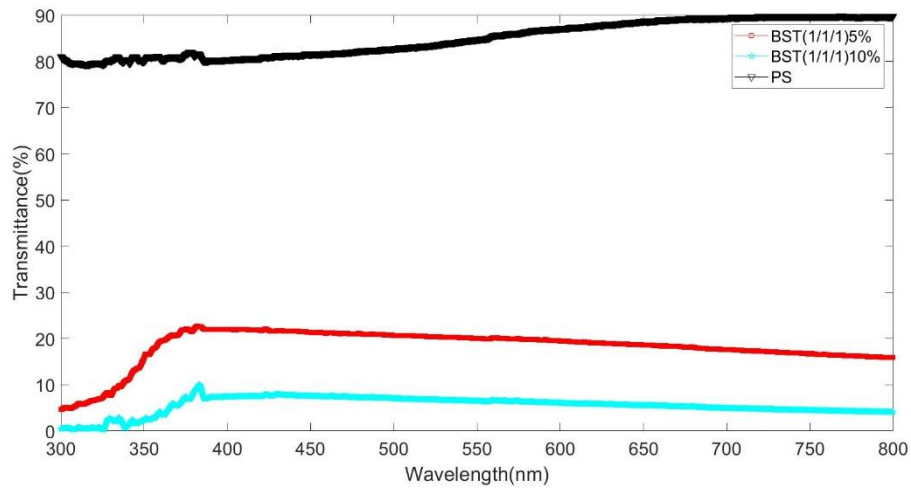


Figure 4.9. Transmittance (%) of pristine PS polymer tape and composites with 5% and 10% as a function of wavelength (for ball milled BST (1/1/1)).

BST (0.7/0.3/1) powders obtained by the centrifugal milling method had smaller average particle sizes. Smaller particle sizes of composites provide more homogeneous distribution in the PS polymer matrix with no agglomeration. Visual appearance and light transmittance of the composites with 5% and 10% centrifugal milled BST (0.7/0.3/1) powders having fine particle size shown in Figure 4.10 and Figure 4.11, respectively, presents similar results, where uniformly distributed fine particles provide more surface coverage and hence lower light transmission through the composites, which is more pronounced with increasing particle content.

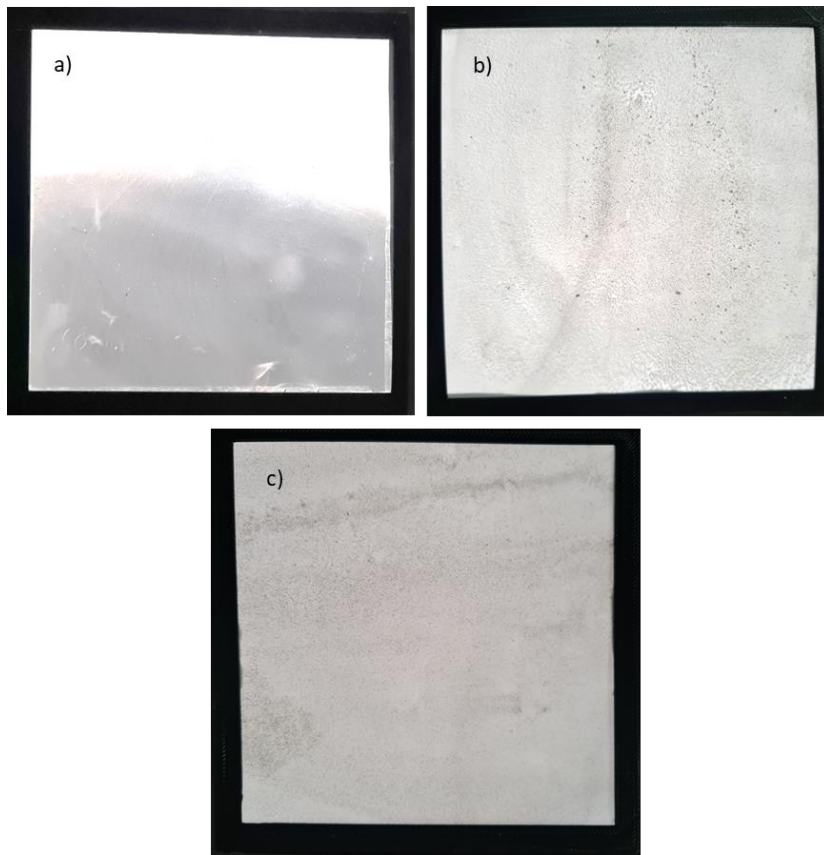


Figure 4.10. Visual appearance of a) pristine PS polymer tape b) composite with 5% BST and c) composite with 10% BST (for centrifugal milled BST (0.7/0.3/1)).

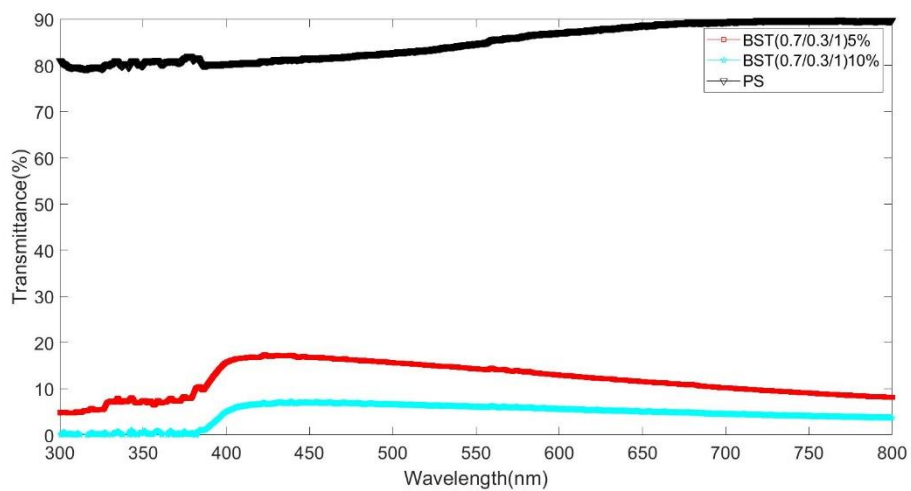


Figure 4.11. Transmittance (%) of pristine PS polymer tape and composites with 5% and 10% as a function of wavelength (for centrifugal milled BST (0.7/0.3/1)).

Visual appearance and light transmittance of the composites with 5% and 10% centrifugal milled BST (1/1/1) powders seem to be similar to each other (Figure 4.12 and Figure 4.13, respectively). As evidenced above, it is expected that higher amount of fine sized BST particle loading should cause darker appearance and lower light transmittance. In this case on the contrary, 10% BST containing composite shows similar light transmittance with 5% BST containing composite. This can be attributed to inhomogeneous distribution of the particles in the PS polymer matrix for this particular case.

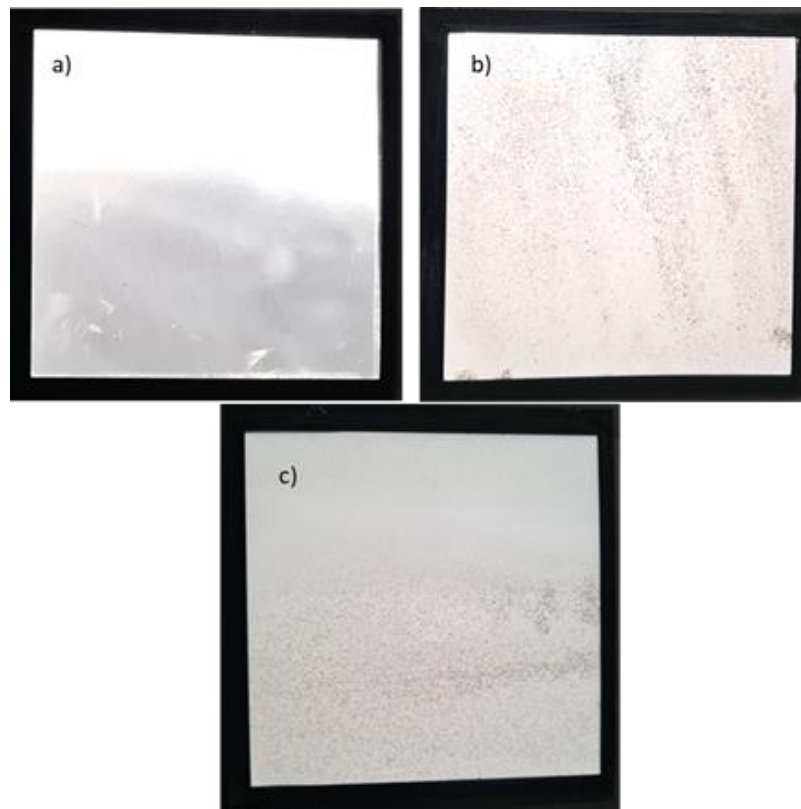


Figure 4.12. Visual appearance of a) pristine PS polymer tape b) composite with 5% BST and c) composite with 10% BST (for centrifugal milled BST (1/1/1)).

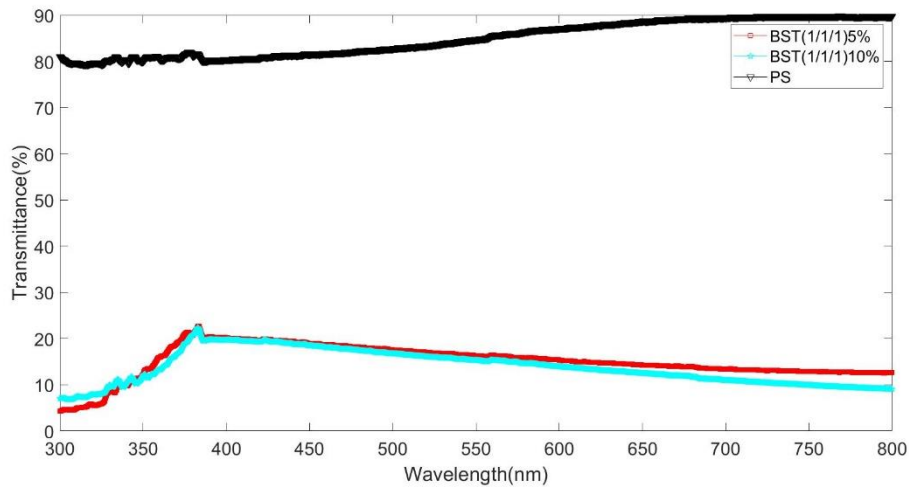


Figure 4.13. Transmittance (%) of pristine PS polymer tape and composites with 5% and 10% as a function of wavelength (for centrifugal milled BST (1/1/1)).

4.5 Dielectric Characterization of BST/PS Composites

Different BST powder contents were used to prepare BST/PS composites. An increase in powder quantity causes the fabricated composites to be more brittle which cannot keep their uniform tape form without cracking during processing. To cope with this problem, powder quantity was limited to a maximum of 10 wt%, and thus, the fabrication of intact composite tapes was achieved. Two different quantities of BST powders were used which were 5 wt% and 10 wt%, respectively. BST powders were produced by two different milling methods and with two different compositions which were used as particles of polymers. Consequently, 8 different set of composites were obtained, and their dielectric properties such as dielectric constant and loss tangent were characterized using free space set up attached to the VNA. Dielectric constant and loss tangent values were extracted using the transmission loss and reflection loss values (S parameters) obtained from the measurements. Transmission loss (S12) versus frequency and reflection loss (S22) versus frequency measurement results of these 8 set of composites are given in Figure 4.14 and Figure 4.15, respectively. Corresponding dielectric constant versus frequency and loss

tangent versus frequency graphs of these composites can be seen in Figure 4.16 and Figure 4.17, respectively.

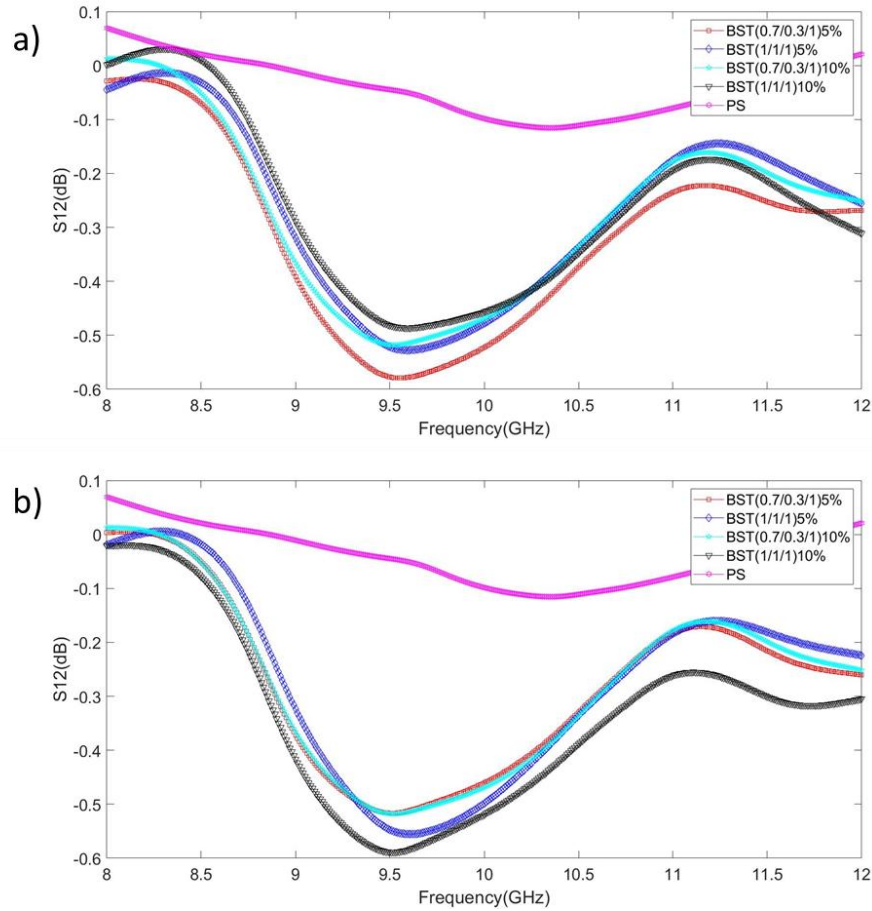


Figure 4.14. Transmission losses (S_{12}) of BST/PS composites with a) ball milled BST powders and b) centrifugal milled BST powders.

Transmission losses of the composites are nearly the same, while pristine monolithic polystyrene shows different pattern from those of the composites. Insertion losses of composites are changing between 0 and -0.6 dB with the peak value observed at 9.5 GHz. This notably low range of transmission losses of the composites shows that incident waves emerging from antenna #2 were almost totally transmitted to antenna #1. While both the composites and the pristine PS show a highly transmitting nature for the electromagnetic (EM) radiation, where that of the pristine PS shows less frequency dependence compared to those of the composites.

Unlike their transmission loss, reflection losses of the composites are relatively different from each other. While pristine PS showed the lowest reflection loss changing between -30 and -32 dB, varying reflection loss patterns were observed for the composites containing ball milled and centrifugal milled BST powders with 2 different compositions. The composite containing 10 wt% BST powder with Ba/Sr/Ti molar ratio of 0.7/0.3/1 shows the highest reflection loss values especially at higher frequencies for both milling methods.

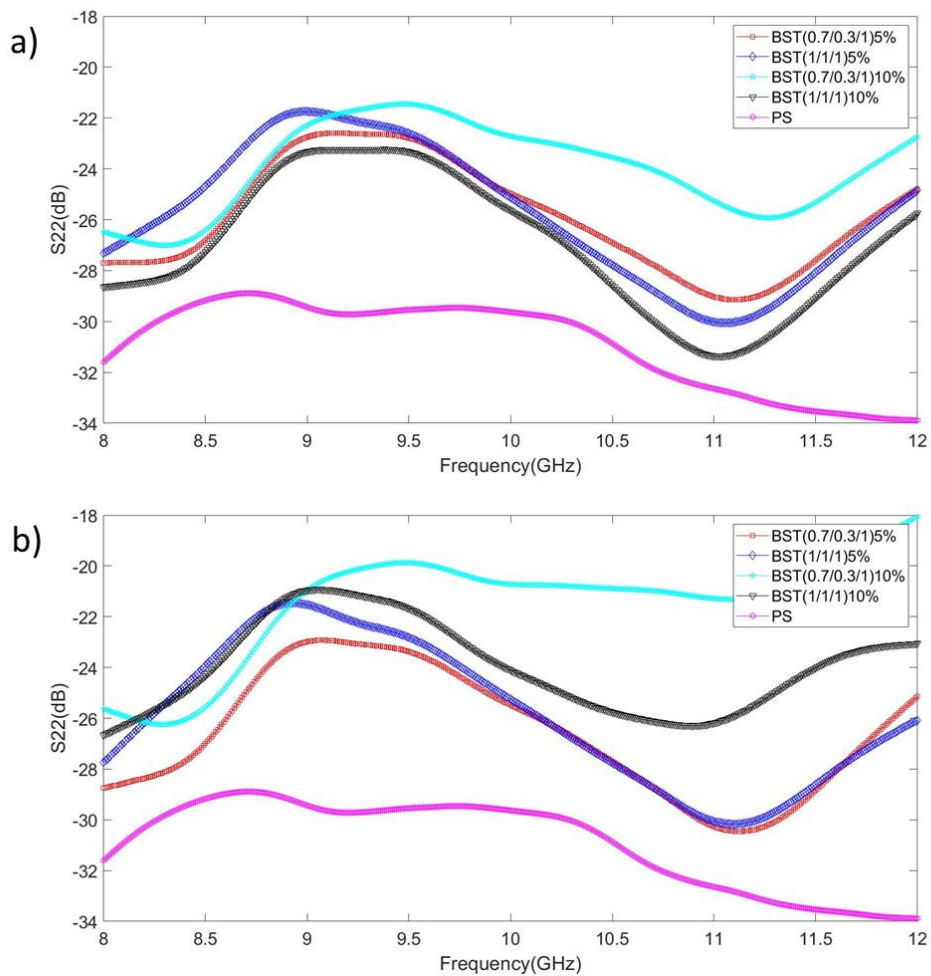


Figure 4.15. Reflection losses (S22) of BST/PS composites with a) ball milled BST powders and b) centrifugal milled BST powders.

Figure 4.16 a) displays dielectric constants of BST/PS composites containing 5 and 10 wt% ball milled BST powders with 2 different compositions. As shown in Figure 4.16, highest dielectric constant reaching to $\sim 1.4-1.8$ was obtained with the composite containing 10 wt% BST having Ba/Sr/Ti molar ratio of 0.7/0.3/1. One of the previous studies, BST/COC composite with 10 wt% BST, had a dielectric constant of 2 at 2-20 GHz [35]. Another study is BST/PPS composites with 30 wt% BST had a dielectric constant of ~ 5 at 1 GHz [3]. Dielectric constant of the composites increases with increasing BST content. In addition to this, Figure 4.16 a) also reveals the effect of BST composition on the dielectric constant of the composites. As mentioned earlier composition is effective on the dielectric constant of BST. At Ba/Sr/Ti molar ratio of 0.7/0.3/1, BST is in the paraelectric phase and has high dielectric constant. However, other compositions do not provide that property, while excess Sr content tends to decrease the dielectric constant of BST [15]. Higher amount of Sr containing compositions are not proper for high dielectric constant at room temperature, as Sr declines dielectric constant because of smaller ionic radius which provides less contribution to the dielectric constant with ionic polarization [16]. In parallel to these explanations, BST with Ba/Sr/Ti molar ratio of 1/1/1 is known to have lower dielectric constant values than BST with 0.7/0.3/1 Ba/Sr/Ti ratio. Consequently, composites containing BST powders with Ba/Sr/Ti molar ratio of 0.7/0.3/1 show higher dielectric constant values (Figure 4.16).

Figure 4.16 b) shows dielectric constants of BST/PS composites containing 5 and 10 wt% centrifugal milled BST powders with 2 different compositions. Centrifugal milling was shown to be superior to ball milling for reducing particle size. A much shorter milling duration is required for the centrifugal milling process to obtain small particle sizes which promote uniform distribution of the powders in the composites. According to dielectric constant models, size and volume fraction of the particles along with their interfacial interaction with the matrix are important parameters in terms of the dielectric constant of the composites. Small particle sizes enhance interfacial polarization of materials [16]. Smaller particle size with good distribution in the matrix provides high dielectric constant values. Therefore, as seen in Figure

4.16 b), composites containing centrifugal milled BST powders with Ba/Sr/Ti molar ratio 0.7/0.3/1 having finer particle size show higher dielectric constant than ball milled BST powders with 0.7/0.3/1 Ba/Sr/Ti ratio.

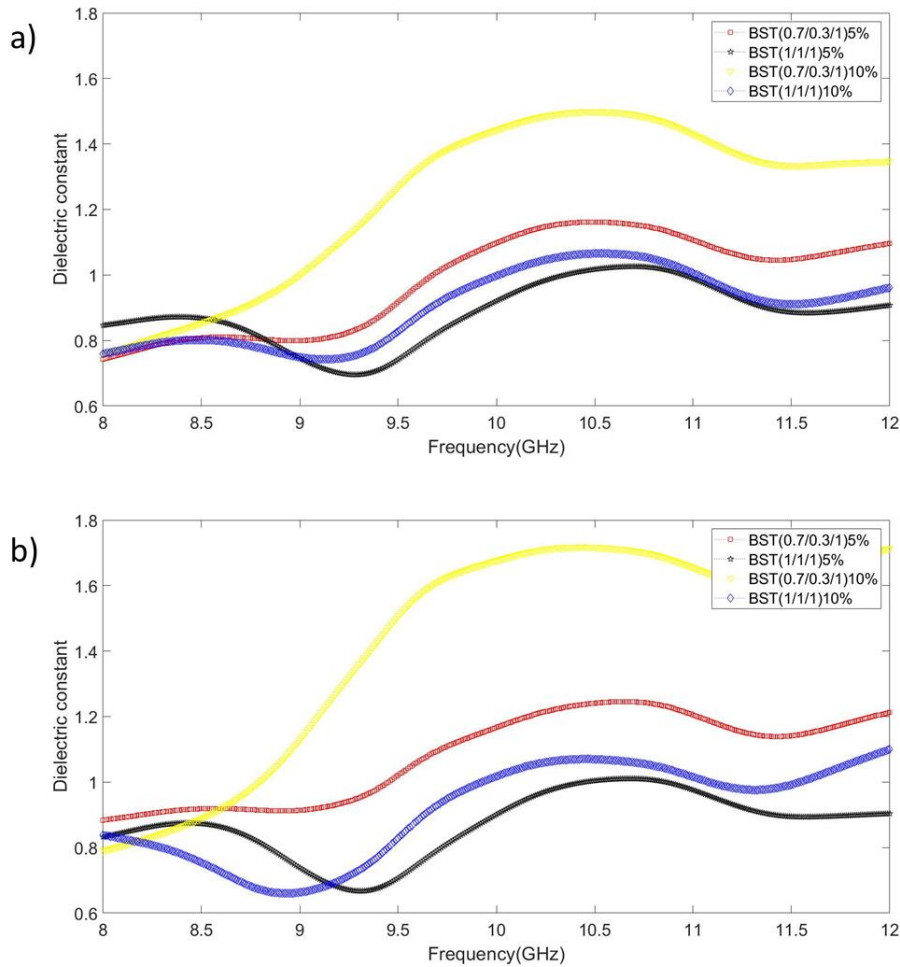


Figure 4.16. Dielectric constants of BST/PS composites with a) ball milled BST powders and b) centrifugal milled BST powders.

Loss tangent values of the composites follow an increasing trend with increasing dielectric constant of the BST powders especially for high dielectric constant values according to literature [15]. At low dielectric constant values, the previous trend does not appear as in this study. Loss tangent values should be as low as possible for efficient operation of electronic devices at high frequencies. According to measurements, composites containing BST powders with Ba/Sr/Ti molar ratio of

1/1/1 have higher loss tangent values compared to the optimum Ba/Sr/Ti molar ratio of 0.7/0.3/1. Among the others the composites containing 10 wt% BST powders with Ba/Sr/Ti molar ratio of 0.7/0.3/1 has the lowest loss tangent values changing between 0.1 and 0.3 in the X-band range. As loss tangent minimization is critical for microwave applications, this composite seems to be the most appropriate one among all of the others for high frequencies.

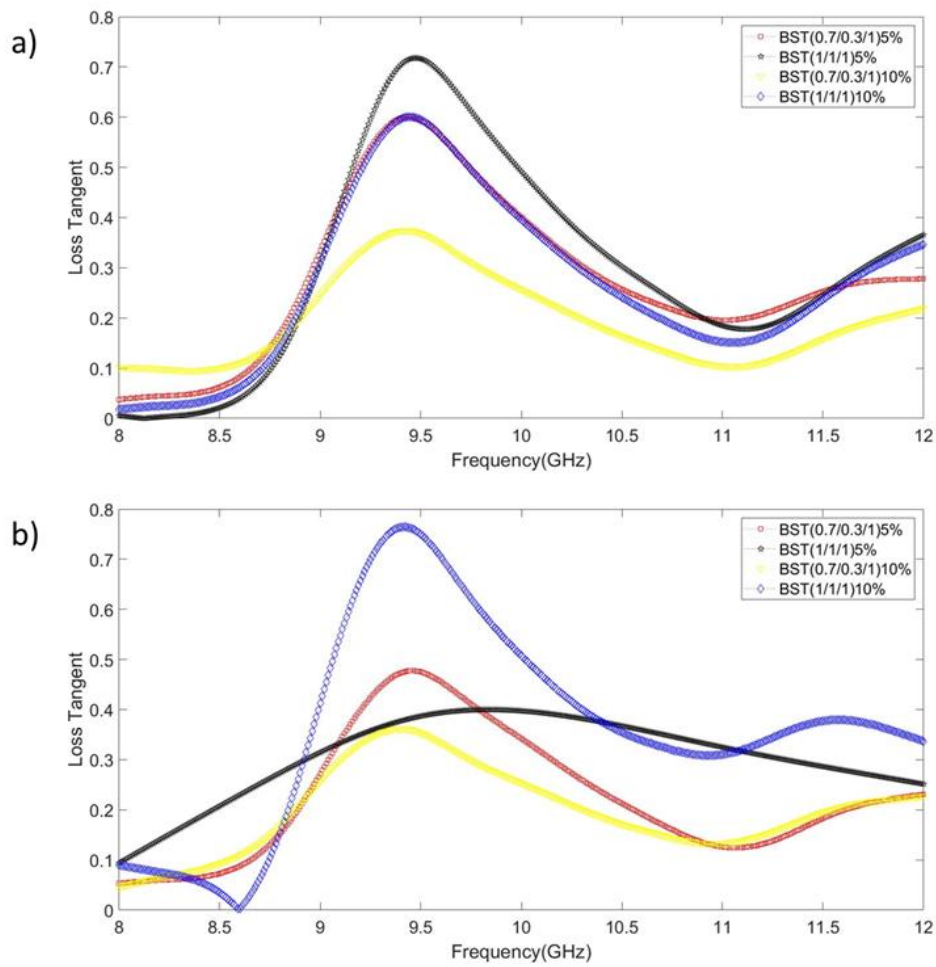


Figure 4.17. Loss tangent of BST/PS composites with a) ball milled BST powders and b) centrifugal milled BST powders.

4.6 Tunability Potential of BST/PS Composites

Demonstration of the tunability potential of the BST containing polymer composites is one of the key points of this study. Materials with low dielectric constant and high tunability have been preferred in recent applications [16]. High tunability values can be obtained with increasing applied bias voltage. Different voltage values were applied to BST/PS composites in this study and change in their reflection loss (S_{22}) was observed.

As shown in Figure 4.18 and Figure 4.19, under applied voltage S_{22} parameters of the BST/PS composites change which means that dielectric constant of BST can also be changed. According to comparison of BST loading in Figure 4.18 and Figure 4.19, 10% BST content provided more change in the S_{22} parameter pointing out to higher tunability potential of the composite. Higher change in the reflection response and hence dielectric properties of the BST particles is expected to provide higher tunability of the material, which is supported by the results of previous studies in the literature [35]. According to previous studies higher interfacial area provides enhancement in interfacial polarization leading to high tunability [49]. Therefore, composites containing finer BST particle sizes are expected to show stronger response to the applied voltage in this study.

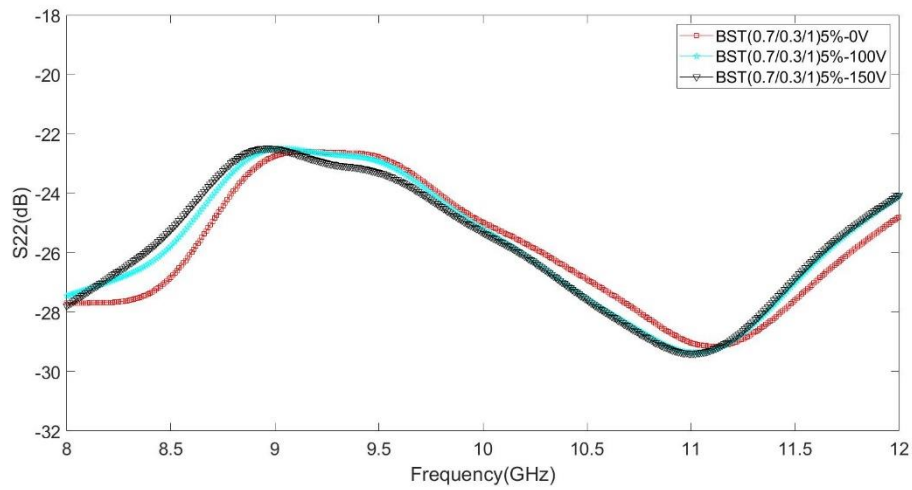


Figure 4.18. Change in reflection loss (S22) of 5 wt% ball milled BST (0.7/0.3/1) containing composite under 0, 100 and 150 V bias voltage.

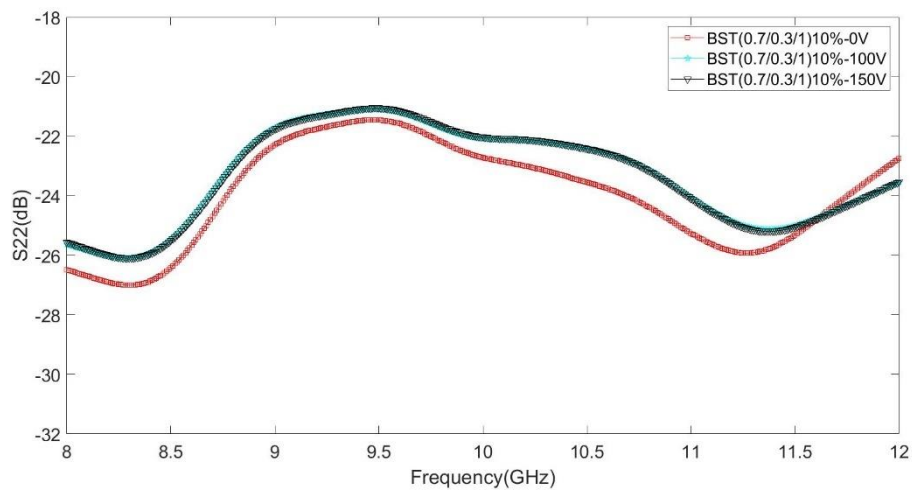


Figure 4.19. Change in reflection loss (S22) of 10 wt% ball milled BST (0.7/0.3/1) containing composite under 0, 100 and 150 V bias voltage.

Figure 4.20 and Figure 4.21 which show the change in reflection loss (S22) of 5 and 10 wt% ball milled BST (1/1/1) containing composite under applied voltage reveals a different pattern than those of the 5 and 10 wt% ball milled BST (0.7/0.3/1) containing composites observed in Figure 4.18 and Figure 4.19. The difference in the change of the reflection response under applied voltage caused by the composition of the BST powders is due to the fact that composition is important on the crystallization and morphology of BST ceramics. $\text{Ba}_{0.67}\text{Sr}_{0.33}\text{TiO}_3$ phase, which

provides a high dielectric constant at room temperature, was not found in BST (1/1/1) composition according to previous XRD analysis. Therefore, the dielectric constant of the composites containing BST powders with this composition is lower. Moreover, irregular shaped and larger particles provided low specific surface area between the polymeric matrix and the particles. Dielectric properties of the composites depend on the interfacial interaction between the polymeric matrix and particles, where poor bonding causes low dielectric constant which results in lower tunability. Lower change in the reflection response of 10 wt% ball milled BST (1/1/1) containing composites displayed lower tunability. Nevertheless, this might have been caused due to the larger size of the agglomerated, ball milled BST (1/1/1) presented previously. The surface area of the particles decreased with agglomeration and weak interfacial interaction and low interfacial polarization area of this BST powder may have lead to the lower response observed.

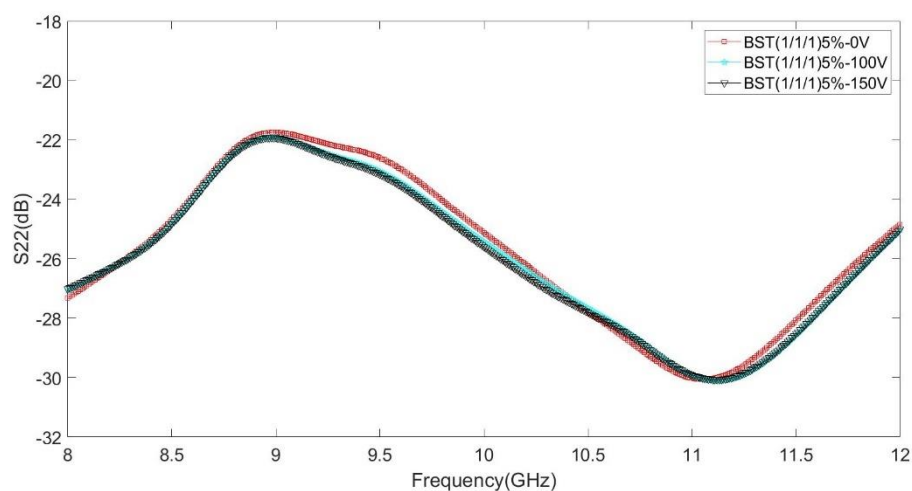


Figure 4.20. Change in reflection loss (S22) of 5 wt% ball milled BST (1/1/1) containing composite under 0, 100 and 150 V bias voltage.

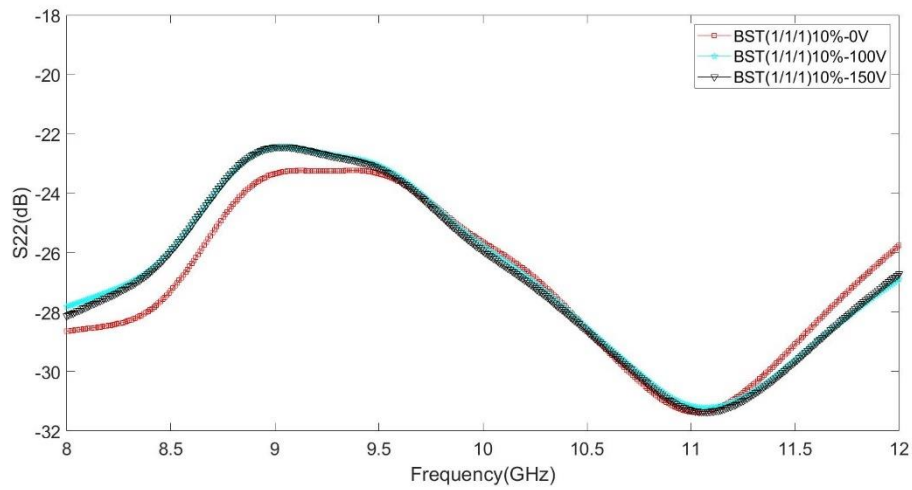


Figure 4.21. Change in reflection loss (S22) of 10 wt% ball milled BST (1/1/1) containing composite under 0, 100 and 150 V bias voltage.

As mentioned before, both ball milled and centrifugal milled BST (0.7/0.3/1) powders show similar dielectric properties. It is known that fine-sized particles are effective on the tunability of BST. Approximately 300 nm sized particles and homogeneous particle distribution without agglomeration in the PS matrix provided the highest change in the reflection response under bias voltage pointing out to the best tunability potential among all of the fabricated composites (Figure 4.22).

At about 8 GHz, the change in the reflection response can be observed clearly for the composite containing 10 wt% centrifugal milled BST (0.7/0.3/1) (Figure 4.23). Increase in frequency causes a decrease in this response. According to the studies available in the literature, tunable materials do not show a linear change with both operating frequencies and applying voltages [35]. Material's permittivity is high at lower frequencies because the excitation of bound electrons, lattice vibration, dipole orientation and charge excitation are active at low frequencies. At higher frequencies, the dielectric properties of the materials show frequency independent behavior [57]. Results of the current study are in accordance with the findings reported in literature.

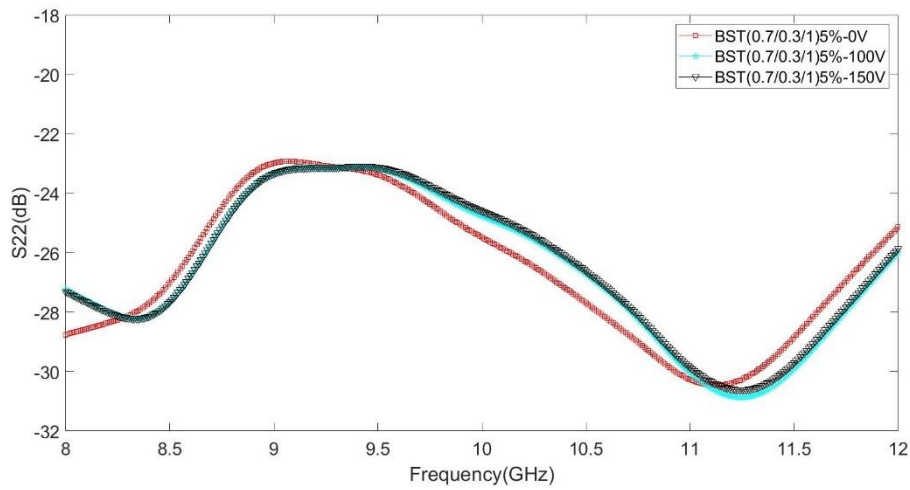


Figure 4.22. Change in reflection loss (S_{22}) of 5 wt% centrifugal milled BST (0.7/0.3/1) containing composite under 0, 100 and 150 V bias voltage.

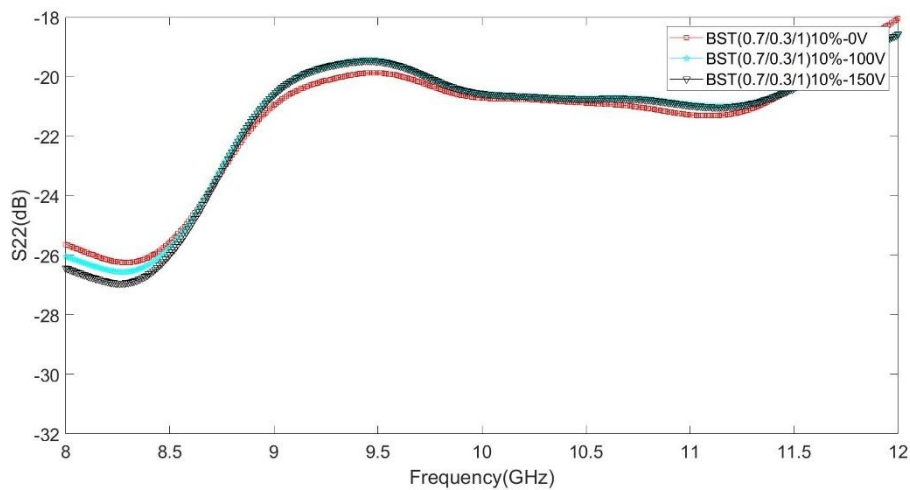


Figure 4.23. Change in reflection loss (S_{22}) of 10 wt% centrifugal milled BST (0.7/0.3/1) containing composite under 0, 100 and 150 V bias voltage.

Figure 4.24 and Figure 4.25 show the change in reflection loss (S_{22}) of 5 and 10 wt% centrifugal milled BST (1/1/1) powder containing composites. Centrifugal milled BST (1/1/1) powder has a small average particle size as other centrifugal milled products. Despite the smaller particle size and homogeneous distribution in the matrix, this composite showed a weak change in the reflection response, as BST (1/1/1) composition is not proper for obtaining required dielectric properties.

Therefore, compared to the composites containing BST (0.7/0.3/1) powders with the optimum composition, the tunability potential of this composite is low.

As shown in Figure 4.25, for the same BST composition reflection response change enhances with increasing BST content in the matrix. Lower BST content causes weaker change in the reflection response, and hence a lower tunability potential is expected. Tunability is a complex behavior of the material. No proper concept is available for varying conditions. Therefore, within the scope of this study it can be concluded that tunability potential of the BST/PS polymer composites improves with increasing content of the fine-sized BST ceramics having Ba/Sr/Ti molar ratio of 0.7/0.3/1 which increases further at higher applied bias voltage.

Results of the experiments are in accordance with the results from previous studies in the sense that the change in reflection losses of the BST/PS composites did not show an only decrease or increase pattern under applied voltage. S22 parameters and also the change in the reflection response show a fluctuating pattern at varying frequencies [51].

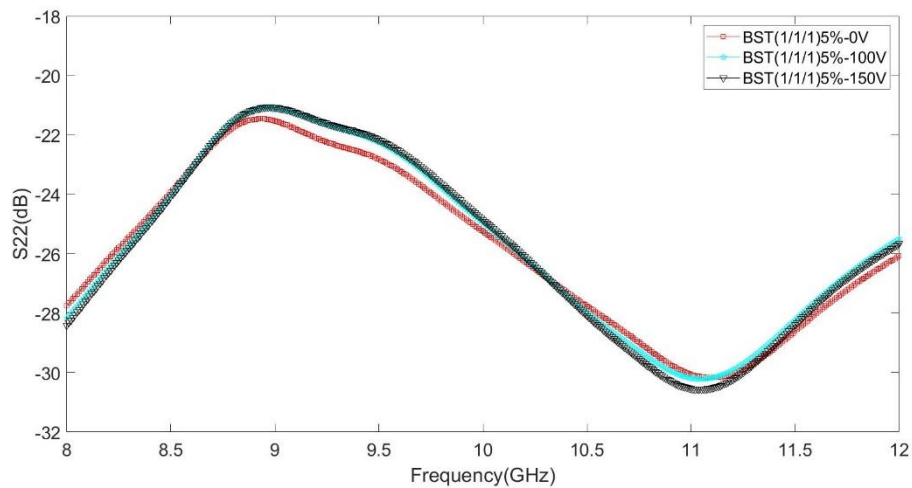


Figure 4.24. Change in reflection loss (S22) of 5% centrifugal milled BST (1/1/1) containing composite under 0, 100 and 150 V bias voltage.

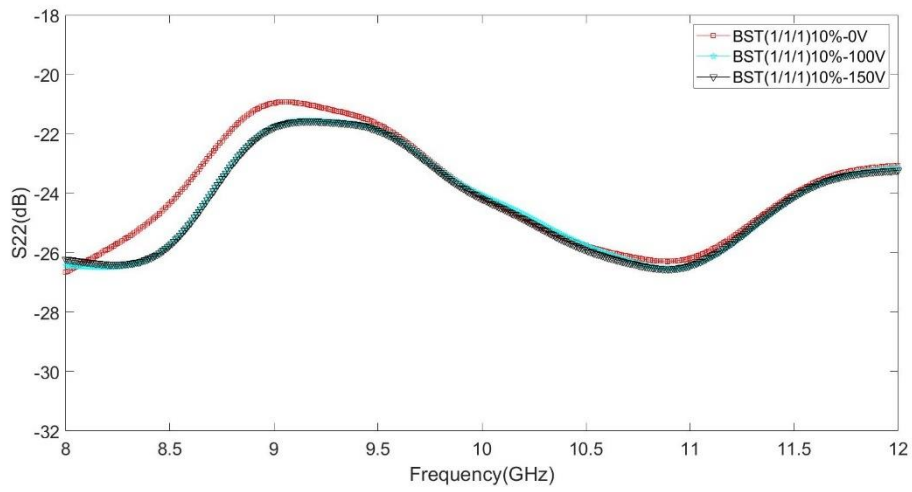


Figure 4.25. Change in reflection loss (S_{22}) of 10% centrifugal milled BST (1/1/1) containing composite under 0, 100 and 150 V bias voltage.

CHAPTER 5

CONCLUSION

In the scope of the present study barium strontium titanate (BST) ferroelectric ceramic particle incorporated polymer matrix composites were investigated for their tunability potentials. Polystyrene type polymeric material was used as the matrix of the composites because of its typical properties such as easy fabrication and desired dielectric properties, which are not found in monolithic BST ceramics. The mixed oxide method based on solid state reaction was used for synthesizing BST particles. Two different milling methods were preferred for mixing and particle size reduction purposes, which are ball milling and centrifugal milling.

Morphological characterization, phase analysis and size analysis of the synthesized BST powders were conducted using with SEM, XRD and particle size analysis. The effects of composition and milling methods on BST morphology, phase formation, particle size, and finally dielectric properties were discussed by evaluating the characterization results.

BST/PS composites were fabricated by tape casting. Response of the composites to the electromagnetic radiation was measured using free space method within the 2-18 GHz frequency range, from which the dielectric properties of the composites such as dielectric constant and loss tangent were extracted. Effects of particle size, distribution and quantity of the BST powders on the dielectric properties of the resulting composites were investigated with the free space measurement method. Optical characterization of fabricated composite tapes was done by UV-VIS spectroscopy. Results of optical characterization provided information about the particle distribution in the composites, which is also effective on their dielectric performance.

Tunability in the dielectric properties of the composites which is a crucial requirement for various microwave devices was measured with the free space measurement method under the application of a bias voltage. Variation in the dielectric constant and loss tangent of the composites under the applied electric field was recorded for investigating the tunability potential of the BST/PS composites.

Following major conclusions have been drawn based on the results of this study:

- Milling methods considerably affect the final particle size, morphology and distribution of the BST powders. Ball milling method takes much longer processing time compared to centrifugal milling in order to achieve comparable powder characteristics.
- Particle size analysis of the BST powders shows that approximately 300 nm of average particle size can be obtained by both milling methods, which is obtained by ball milling durations in the order of hours, whereas it was obtained by centrifugal mixing durations in the order of minutes. However, ball milling is prone to cause agglomeration resulting in deterioration in particle size distribution.
- SEM investigation of the synthesized powders displayed spherical morphology of particles especially for the Ba/Sr/Ti molar ratio of 0.7/0.3/1. Variation in particle morphology has been observed for two different milling methods. Powders obtained by ball milling have some deviation from the spherical shape.
- Another obvious result of the SEM investigation is that powders with the Ba/Sr/Ti molar ratio of 1/1/1 are not completely spherical for both milling methods. Agglomeration was detected particularly for this composition.

- X-ray diffraction analysis revealed the phase constitution of the synthesized powders. In the powder with a Ba/Sr/Ti molar ratio of 0.7/0.3/1 $\text{Ba}_{0.67}\text{Sr}_{0.33}\text{TiO}_3$ phase was formed. In the case of centrifugal milled powders high intensity peaks of the $\text{Ba}_{0.67}\text{Sr}_{0.33}\text{TiO}_3$ phase were obtained closely matching to the peaks of the reference. On the other hand, ball milling of the same composition resulted in weaker peak intensities where the peaks slightly deviate to the higher angles.

- It was observed that in the powder with a Ba/Sr/Ti molar ratio of 1/1/1 $\text{Ba}_{0.67}\text{Sr}_{0.33}\text{TiO}_3$ phase was not formed. Instead of the BST phase, Barium titanate and Strontium titanate phases were formed.

- UV-VIS spectrophotometer measurements were conducted on the BST/PS composite tapes. Results show that presence of high quantity of BST particles in the PS matrix causes lower light transmission. Even though slightly there exists some ambiguities in the light transmission of 5 wt% and 10 wt% BST powder containing composites. These deviations are proof of agglomeration and inhomogeneous particle size distribution depending on the composition of the BST powders along with the milling method utilized.

- Composites containing BST powders with a Ba/Sr/Ti molar ratio of 0.7/0.3/1 showed optimum dielectric properties. At this optimum composition, BST has the highest dielectric constant, which has also been verified by other studies in the literature. Besides this, for this composition increasing the amount of BST particles in the matrix enhanced the dielectric properties of the composites.

- Composites containing BST powders with Ba/Sr/Ti molar ratio of 1/1/1 contained agglomerations. In addition to agglomerations, Ba/Sr/Ti molar ratio of 1/1/1 did not provide highest dielectric constant at room

temperature. Therefore, composites containing BST powders with Ba/Sr/Ti molar ratio of 1/1/1 had lower dielectric constant and higher loss tangent compared to composites with BST powders having the optimum composition. Even though this the case, increase in dielectric constant of the composite was also observed with increasing amount of the BST powders with this composition.

- Dielectric characterization also showed that composites containing centrifugal milled BST powders had higher dielectric constant compared to those containing ball milled ones.
- Loss tangent values of the composites decrease with increasing dielectric constants of the composites according to experimental results.
- Optimum dielectric properties which are highest dielectric constant and lowest loss tangent were obtained in the composite containing 10 wt% of centrifugal milled BST powders with a Ba/Sr/Ti molar ratio of 0.7/0.3/1.
- Tunability measurements of the composites revealed diverse results. Composites containing 10% of ball milled BST powders with a Ba/Sr/Ti molar ratio of 0.7/0.3/1 having the highest dielectric constant also revealed the highest value of tunability. Lower dielectric constant of the composite with 5 wt% of the same BST powder led lower tunability.
- On the other hand, in the case of composites containing centrifugal milled BST powders with a Ba/Sr/Ti molar ratio of 0.7/0.3/1, lower amount of BST powders of 5 wt% in the composite provided higher tunability than composites with 10 wt% BST. High dielectric constant does not necessarily bring about high tunability all the time. Nanosized particles have different distributions in the composites, while agglomeration of particles is highly

possible. Local agglomerations can be present in the composites, which might have caused this ambiguity between the dielectric constant value and the level of tunability. Moreover, tunability is a complicated concept which is not dependent on a single parameter. Frequency or applied voltage values are also effective on tunability of the dielectric properties.

- Ball milled BST powders with a Ba/Sr/Ti molar ratio of 1/1/1 has larger average particle size and many agglomerations. Consequently, tunability of 5 wt% BST containing composite is more than that of 10 wt% BST containing one because of agglomeration of large particles.

- The tunability of the composites containing centrifugal milled BST powders with a Ba/Sr/Ti molar ratio of 1/1/1 is similar for both 5% and 10% powder content. Agglomeration resulted inhomogeneous distribution of the BST powders might have caused variation in tunability at different frequencies for these two composites.

- Overall evaluation of the tunability measurements showed that there is no significant difference in the tunability of the BST/PS composites at the applied bias voltage of 100 V and 150 V.

REFERENCES

- [1] F.W. Jamaluddin, M.F. Abdul Khalid, M.K.A. Mahmood, M. H. Mamat, A.S. Zoolfakar, Surface Morphological, Topological and Crystallinity Characteristics of Sputtered Barium Strontium Titanate Thin Films on Sapphire Substrates, *Int. Journal of Electrical and Electronic Systems Research*, 15 (2019) 60–65.
- [2] L. Gao, Z. Guan, S. Huang, K. Liang, H. Chen, J. Zhang, Enhanced Dielectric Properties of Barium Strontium Titanate Thin Films by Doping Modification, *Journal of Materials Science: Materials in Electronics*, 30 (2019) 12821–12839.
- [3] T. Hu, J. Juuti, H. Jantunen, RF Properties of BST-PPS Composites, *Journal of the European Ceramic Society*, 27 (2007) 2923–2926.
- [4] T. Hu, J. Juuti, H. Jantunen, T. Vilkmann, Dielectric Properties of BST/polymer Composite, *Journal of the European Ceramic Society*, 27 (2007) 3997–4001.
- [5] Z. Saroukhani, N. Tahmasebi, S.M. Mahdavi, A. Nematy, Effect of Working Pressure and Annealing Temperature on Microstructure and Surface Chemical Composition of Barium Strontium Titanate Films Grown by Pulsed Laser Deposition, *Bull. Mater. Sci.*, 38 (2015) 1645–1650.
- [6] M.W. Cole, R.G. Geyer, Novel Tunable Acceptor Doped BST Thin Films for High Quality Tunable Microwave Devices, *Revista Mexicana De Fisica*, 50 (2004) 232–238.
- [7] R. E. Hummel, *Electronic Properties of Materials*, Third Edition, Springer, (2000).

- [8] N. Izyumskaya, Y. I. Alivov, S. J. Cho, H. Morkoç, H. Lee, Y. S. Kang, Processing, Structure, Properties, and Applications of PZT Thin Films, *Critical Reviews in Solid State and Materials Sciences*, 32 (2007) 111–202.
- [9] Y. Zheng, Tunable Multiband Ferroelectric Devices for Reconfigurable RF-Frontends, in: LNEE, Springer, (2013).
- [10] B. Jaffe, W. R. Cook, H. Jaffe, *Piezoelectric Ceramics*, London: Academic Press, (1971).
- [11] R. Stanculescu, C.E. Ciomaga, L. Padurariu, P. Galizia, N. Horchidan, C. Capiani, C. Galassi, L. Mitoseriu, Study of The Role of Porosity on the Functional Properties of (Ba,Sr)TiO₃ Ceramics, *Journal of Alloys and Compounds*, 643 (2015) 79–87.
- [12] R.B. Upadhyay, S. Annam, M.R. Patel, U.S. Joshi, Influence of Aliovalent Doping on Dielectric Properties of Ba_{0.6}Sr_{0.4}TiO₃ Thin Film for Voltage Tunable Applications, *Integrated Ferroelectrics*, 167 (2015) 184–191.
- [13] M. Zhang, J. Zhai, B. Shen, X. Yao, MgO Doping Effects on Dielectric Properties of Ba_{0.55}Sr_{0.45}TiO₃ Ceramics, *Journal of the American Ceramic Society*, 94 (2011) 3883–3888.
- [14] L. Nedelcu, M. I. Toacsan, M. G. Banciu, A. Ioachim, Dielectric Properties of Paraelectric Ba_{1-x}Sr_xTiO₃ Ceramics, *Ferroelectrics*, 391 (2009) 33–41.
- [15] E.A. Nenasheva, N.F. Kartenko, I.M. Gaidamaka, S.S. Redozubov, A.B. Kozyrev, A.D. Kanareykin, Low Permittivity Ferroelectric Composite Ceramics for Tunable Applications, *Ferroelectrics*, 506 (2017) 174–183.
- [16] F. Gao, K. Zhang, Y. Guo, J. Xu, M. Szafran, (Ba, Sr)TiO₃/Polymer Dielectric Composites–Progress and Perspective, *Progress in Materials Science*, 121 (2021) 100813.

- [17] S. Aymen, M. Mascot, F. Jomni, J.C. Carru, High Tunability in Lead-free Ba_{0.85}Sr_{0.15}TiO₃ Thick Films for Microwave Tunable Applications, *Ceramics International*, 45 (2019) 23084–23088.
- [18] A. Jamaluddin, Suwarni, A. Supriyanto, Y. Iriani, Properties of Strontium Doped Barium Titanate Powder Prepared by Solid State Reaction, *Journal of Physics: Conference Series*, 776 (2016).
- [19] Q. Wang, P. Ren, L. Sun, H. Jin, G. Zhao, Microstructure and Tunable Dielectric Properties of Ba_{0.6}Sr_{0.4}TiO₃/Y₂O₃ Composite Ceramics, *Journal of Materials Science*, 51 (2016) 6249–6256.
- [20] H. Zhang, H. Giddens, Y. Yue, X. Xu, v. Araullo-Peters, v. Koval, M. Palma, I. Abrahams, H. Yan, Polar Nano-Clusters in Nominally Paraelectric Ceramics Demonstrating High Microwave Tunability for Wireless Communication, *Journal of the European Ceramic Society*, 40 (2020) 3996–4003.
- [21] J.W. Liou, B.S. Chiou, Dielectric Tunability of Barium Strontium Titanate/Silicone-Rubber Composite, *Journal of Physics: Condensed Matter*, 10 (1998) 2773–2786.
- [22] R. Dewi, Formation and Characterization of Typical Films Ba_{0.2}Sr_{0.8}TiO₃ Using XRD, FESEM and Spectroscopy Impedance, *Journal of Physics: Conference Series*, 1120 (2018).
- [23] R. Dewi, K. Krisman, Z. Zulkarnaen, R. A. Syahraini, TS L. Husein, The Determination of Barium Strontium Titanate Thin Film Band Gap Energy Ba_{0.15}Sr_{0.85}TiO₃ Using Ultraviolet-Visible Spectroscopy, *SPEKTRA: Jurnal Fisika Dan Aplikasinya*, 5 (2020) 11–20.
- [24] M. Y. Shahid, A. Anwar, F. Malik, M. Asghar, M. F. Warsi, S. Z. Ilyas, Effect of Sr-Doping on Ferroelectric and Dielectric Properties of Sol-Gel Synthesized BaTiO₃ Thin Films, *Digest Journal of Nanomaterials and Biostructures*, 12 (2017) 669–677.

- [25] D. Levasseur, H.B. El-Shaarawi, S. Pacchini, A. Rousseau, S. Payan, G. Guegan, M. Maglione, Systematic Investigation of the Annealing Temperature and Composition Effects on the Dielectric Properties of Sol-gel $\text{Ba}_x\text{Sr}_{1-x}\text{TiO}_3$ Thin Films, *Journal of the European Ceramic Society*, 33 (2013) 139–146.
- [26] C. Chen, A. Wei, Y. Li, K. Zhou, D. Zhang, Improved Tunable Properties of Co Doped $\text{Ba}_{0.8}\text{Sr}_{0.2}\text{TiO}_3$ Thin Films Prepared by Sol-gel Method, *Journal of Alloys and Compounds*, 692 (2017) 204–211.
- [27] R. Dewi, Optical Characterization of $\text{Ba}_{1-x}\text{Sr}_x\text{TiO}_3$ Thin Film Properties Using Ultraviolet-Visible Spectroscopy, *AIP Conference Proceedings*, 2219(1) (2020).
- [28] Y. Wang, S. C. Yue, F. L. Mao, Y. Jia, H. Zhang, Researches on Enhancement of Dielectric Performance of Two-layer BST Films, *Proceedings of the 2020 15th Symposium on Piezoelectricity, Acoustic Waves and Device Applications*, (2021) 508–511.
- [29] R. Gupta, v. Gupta, M. Tomar, Structural and Dielectric Properties of PLD Grown BST Thin Films, *Vacuum*, 159 (2019) 69–75.
- [30] A. Selmi, O. Khaldi, M. Mascot, F. Jomni, J.C. Carru, High-Performance Screen-Printed $\text{Au}/\text{Ba}_{0.85}\text{Sr}_{0.15}\text{TiO}_3/\text{Pt}$ Capacitors for Tunable Devices, *Journal of Alloys and Compounds*, 878 (2021) 160340.
- [31] O.K. Ranasingha, M. Haghzadeh, M.J. Sobkowicz, E. Kingsley, C. Armiento, A. Akyurtlu, Formulation and Characterization of Sinterless Barium Strontium Titanate (BST) Dielectric Nanoparticle Ink for Printed RF and Microwave Applications, *Journal of Electronic Materials*, 50 (2021) 3241–3248.
- [32] M. Haghzadeh, C. Armiento, A. Akyurtlu, Fully Printed Varactors and Phase Shifters Based on a BST/Polymer Ink for Tunable Microwave Applications, *2016 IEEE MTT-S International Microwave Symposium (IMS)*, (2016) 1–4.

- [33] D. Gao, Z. Tan, Z. Fan, M. Guo, Z. Hou, D. Chen, M. Qin, M. Zeng, G. Zhou, X. Gao, X. Lu, J.M. Liu, All-Inorganic Flexible Ba_{0.67}Sr_{0.33}TiO₃ Thin Films with Excellent Dielectric Properties over a Wide Range of Frequencies, *ACS Applied Materials and Interfaces*, 11 (2019) 27088–27097.
- [34] M. Haghzadeh, H. Jaradat, C. Armiento, A. Akyurtlu, Design and Simulation of Fully Printable Conformal Antennas with BST/Polymer Composite Based Phase Shifters, *Progress In Electromagnetics Research C*, 62 (2016) 167–178.
- [35] E. Hajisaeid, M. Haghzadeh, M. Shone, P. Mooney, A. Panwar, C. Barry, J. Mead, C. Armiento, A. Akyurtlu, Printed Tunable Frequency Selective Surface on a Developed Flexible Functionalized Ceramic-Polymer Based Substrate, 2016 IEEE International Symposium on Phased Array Systems and Technology (PAST), (2016) 1–5.
- [36] M. Teirikangas, J. Juuti, H. Jantunen, Multilayer BST-COC Composite with Enhanced High Frequency Dielectric Properties, *Ferroelectrics*, (2009) 210–215.
- [37] K. Zhang, F. Gao, J. Xu, L. Wang, Q. Zhang, J. Kong, Fabrication and Dielectric Properties of Ba_{0.6}Sr_{0.4}TiO₃ / Acrylonitrile–Butadiene–Styrene Resin Composites, *Journal of Materials Science: Materials in Electronics*, 28 (2017) 8960–8968.
- [38] E. Hajisaeid, S. Deshmukh, S.J. Burbine, E.E. Keaney, C. Lepont, M. Herndon, C. Barry, J. Mead, A. Akyurtlu, Printed Planar Tunable Composite Right/Left-Handed Leaky-Wave Antenna Based on a Tunable Polymer-BST Substrate, *Microwave and Optical Technology Letters*, 63 (2021) 626–637.
- [39] K. Godziszewski, Y. Guo, Y. Yashchyshyn, F. Gao, BST/PVDF Ferroelectric Composites Characteristics at Microwave Frequencies, 2020 23rd International Microwave and Radar Conference (MIKON), (2020) 95–98.
- [40] G. Hu, F. Gao, J. Kong, S. Yang, Q. Zhang, Z. Liu, Y. Zhang, H. Sun, Preparation and Dielectric Properties of Poly(vinylidene

- fluoride)/Ba_{0.6}Sr_{0.4}TiO₃ Composites, *Journal of Alloys and Compounds*, 619 (2015) 686–692.
- [41] S. Shalu, P. Kar, J. Krupka, B. Dasgupta Ghosh, Synthesis, Characterization, Thermal, Dynamic Mechanical, and Dielectric Studies of Ba_{0.7}Sr_{0.3}TiO₃/Polystyrene Composites, *Polymer Composites*, 39 (2018) E1714–E1724.
- [42] D. Walk, P. Salg, D. Kienemund, A. Radetinac, L. Zeinar, C. Schuster, P. Komissinskiy, L. Alff, R. Jakoby, H. Maune, Characterization and Modeling of Epitaxially Grown BST on a Conducting Oxide Electrode, *Proceedings of the 48th European Microwave Conference*, (2018) 563–566.
- [43] Y. Shen, S. Ebadi, P. Wahid, X. Gong, Tunable and Flexible Barium Strontium Titanate (BST) Varactors on Liquid Crystal Polymer (LCP) Substrates, *2012 IEEE/MTT-S International Microwave Symposium Digest.*, (2012) 1–3.
- [44] A. Friederich, C. Kohler, M. Nikfalazar, A. Wiens, M. Sazegar, R. Jakoby, W. Bauer, J.R. Binder, Microstructure and Microwave Properties of Inkjet Printed Barium Strontium Titanate Thick-Films for Tunable Microwave Devices, *Journal of the European Ceramic Society*, 34 (2014) 2925–2932.
- [45] J. Xu, W. Menesklou, E. Ivers-Tiffée, Processing and Properties of BST Thin Films for Tunable Microwave Devices, *Journal of the European Ceramic Society*, 24 (2004) 1735–1739.
- [46] S. Pacchini, A. Rousseau, B. Ouagague, H. B. El-Shaarawy, S. Pacchini, S. Payan, A. Rousseau, M. Maglione, R. Plana, BST Tunability Study at DC and Microwave Frequencies by Using IDC and MIM Capacitors, *2010 Asia-Pacific Microwave Conference*, (2010) 1837–1840.
- [47] M. Nikfalazar, A. Mehmood, M. Sohrabi, A. Wiens, Y. Zheng, H. Maune, R. Jakoby, M. Mikolajek, A. Friederich, C. Kohler, J. R. Binder, Low Bias Voltage Tunable Phase Shifter Based on Inkjet-Printed BST MIM Varactors

- for C/X-Band Phased Arrays, 2015 European Microwave Conference (EuMC), (2015) 1264–1267.
- [48] M. Haghzadeh, A. Akyurtlu, All-printed, flexible, reconfigurable frequency selective surfaces, *Journal of Applied Physics*, 120 (2016).
- [49] M. Haghzadeh, C. Armiento and A. Akyurtlu, All-Printed Flexible Microwave Varactors and Phase Shifters Based on a Tunable BST/Polymer, *IEEE Transactions on Microwave Theory and Techniques*, 65(6) (2017) 2030-2042.
- [50] J. Nath, D. Ghosh, J. P. Maria, A. I. Kingon, W. Fathelbab, P. D. Franzon, M. B. Steer, An Electronically Tunable Microstrip Bandpass Filter Using Thin-Film Barium-Strontium-Titanate (BST) Varactors, *IEEE Transactions on Microwave Theory and Techniques*, (2005) 2707–2712.
- [51] S. Kumar, C. S. Yadav, B. Mali, Design of Microstrip Tunable Bandpass Filter using Ferroelectric Thin Film Varactor, 2020 International Conference on Computational Performance Evaluation (ComPE), (2020) 826-830.
- [52] H. V. Nguyen, A. Sharaiha, Design of Miniaturized and Tunable Antenna by Integrating BST Thin Film Varactor, 2018 International Conference on Advanced Technologies for Communications (ATC), (2018) 65-68.
- [53] D. Zhang, W. Hu, C. Meggs, B. Su, T. Price, D. Iddles, M. J. Lancaster, T. W. Button, Fabrication and Characterisation of Barium Strontium Titanate Thick Film Device Structures for Microwave Applications, *Journal of the European Ceramic Society*, 27 (2007) 1047–1051.
- [54] A.M. Nicolson, G.F. Ross, Measurement of the Intrinsic Properties of Materials by Time-Domain Techniques, *IEEE Transactions on Instrumentation and Measurement*, 19(4) (1970) 377-382.

- [55] W.B. Weir, Automatic Measurement of Complex Dielectric Constant and Permeability at Microwave Frequencies, Proceedings of the IEEE, 62(1) (1974) 33-36.
- [56] E.J. Rothwell, J.L. Frasc, S.M. Ellison, P. Chahal, R.O. Ouedraogo, Analysis of the Nicolson-Ross-Weir Method for Characterizing the Electromagnetic Properties of Engineered Materials, Progress In Electromagnetics Research, 157 (2016) 31-47.
- [57] R.J. Pandya, U.S. Joshi, O.F. Caltun, Microstructural and Electrical Properties of Barium Strontium Titanate and Nickel Zinc Ferrite Composites, Procedia Materials Science, 10 (2015) 168–175.